mechanism of toxicity causing cholestatic injury of the biliary canaliculi or bile ducts. To identify putative metabolites associated with cholestasis, urine samples obtained were subjected to ^{1}H nuclear magnetic resonance analysis.

Previous studies using various types of hepatotoxicants (4,4′-methylene dianiline, clofibrate and galactosamine) suggested that urinary metabolites with chemical shifts of 0.66 to 1.90 ppm were markedly affected by 4,4′-methylene dianiline [12], which is known to induce cholestasis. The dose of 4,4′-methylene dianiline, 250 mg/kg, oral administration, in one previous study was relatively high and might have injured tissues other than the liver [27]. In the present study, area intensities of proton signals from 0.66 to 1.90 ppm (table 2) increased after 4,4′-methylene dianiline treatment in a dose-dependent manner from 50 mg/kg, oral administration (fig. 2), reproducing the findings of previous studies. These results imply that the observed changes in proton signals from 0.66 to 1.90 ppm are closely related to cholestasis. α-Naphthylisothiocyanate is a well-known cholestatic hepatotoxicant and produces cholestasis through injury of epithelial cells of the major bile duct [28]. α-Naphthylisothiocyanate is reported to cause liver injury by a mechanism different from that of 4,4′-methylene dianiline [29], and some differences between 4,4′-methylene dianiline and α-naphthylisothiocyanate treatment may support this (tables 4 and 5). Even if differences do exist in hepatotoxic mechanism between 4,4′-methylene dianiline and α-naphthylisothiocyanate, the two agents produced the same urinary metabolite pattern, suggesting that the changes in urinary metabolites observed were caused by cholestasis itself. The results for α-naphthylisothiocyanate agree with those of previous studies by Beckwith-Hall *et al.* (200 mg/kg, oral administration), Waters *et al.* (150 mg/kg, oral administration), and Schoonen *et al.* (100 mg/kg, oral administration), who reported that bile acids, valine, isoleucine, leucine, and creatine levels were increased in urine [8,30,31]. α-Naphthylisothiocyanate impairs bile flow, resulting in accumulation of bile acids within the bile ducts, and this may lead to bile acid-mediated micellar solubilization of membrane lipids due to a detergent effect in experimental animals [32].

Artificial cholestasis producing permanent obstruction of bile flow has been induced by bile duct ligation [33] and compared with cholestasis induced by chemical substances in rats. Persistent increases in γ-glutamyltranspeptidase, total bilirubin and urinary valine and methyl malonate indicated permanent stasis of bile flow and agreed with a study revealing increase in urinary excretion of bile acids in bile duct ligation-treated rats [34]. Since the change in urinary metabolite profile at 0.66 to 1.90 ppm in the 4,4′-methylene dianiline- and α-naphthylisothiocyanate-treated groups are quite similar to that in animals with bile duct ligation (fig. 5B, D and F), 4,4′-methylene dianiline and α-naphthylisothiocyanate appear to induce cholestasis by obstructing bile flow and thus produce urinary metabolite patterns similar to those obtained with bile duct ligation. As shown in table 5 and fig. 4, although some differences existed among treatments in urinary metabolites, the patterns of changes were not consistent among 4,4′-methylene dianiline, α-naphthylisothiocyanate and bile duct ligation, suggesting that these changes are not specific to cholestasis.

Cyclosporine A was used to inhibit biliary secretion of bile acid, as cyclosporine A is known to cause cholestasis by inhibiting both basal and canalicular hepatocellular bile salt transporters [35,36] and suppressing the bile flow. Although no remarkable histological changes were observed in the cyclosporine A-treated group (table 4), functional impairment of cells in the biliary canaliculi appeared to be induced, as suggested by the increase in serum total bilirubin and total bile acids with cyclosporine A at both 10 and 20 mg/kg. There have also been reports that administration of cyclosporine A at the same doses resulted in significant decrease in bile flow and bile acid secretion [14–16]. Therefore, cyclosporine A was considered to have produced cholestasis as with 4,4′-methylene dianiline, α-naphthylisothiocyanate and bile duct ligation. However, in urinary metabolites, cyclosporine A differed markedly from 4,4′-methylene dianiline, α-naphthylisothiocyanate and bile duct ligation in that it decreased the area intensities of proton signals from 0.66 to 1.90 ppm in urine (fig. 5A, C and E).

The change of urinary metabolites induced by cyclosporine A may be caused by nephrotoxicity, because histological changes characterized by tubular degeneration of the kidneys were noted in the cyclosporine A-treated group (table 4). However, this possibility is not plausible because the characteristic changes of nephrotoxicity in urinary metabolites were not observed in this study. Cyclosporine A is known to injure the proximal tubule cells in rats [37,38]. In previous studies using cyclosporine A at a dose of 45 mg/kg and oral administration for 9 days, Lenz *et al.* reported increases of glucose, acetate, succinate, trimethylamine, lactate, and decreases of citrate, trimethylamine-*N*-oxide [18]. Other nephrotoxic compounds, including hexachlorobutadiene, mercuric chloride, para-aminophenol, sodium fluoride, and uranyl nitrate, which induce the proximal tubule cell injury, are also shown to increase glucose, acetate, succinate, amino acids (alanine, isoleucine, leucine, valine), lactate, *N,N*-dimethylglycine and decrease citrate, 2-oxyglutarate and hippurate in urine by ^{1}H nuclear magnetic resonance analysis [39–43]. Therefore, cyclosporine A at 45 mg/kg, oral administration, is considered to induce changes in urinary metabolites due to nephrotoxicity. However, in the present study, cyclosporine A at 10 and 20 mg/kg, intraperitoneal administration did not increase acetate, succinate, trimethylamine, lactate, nor decrease trimethylamine-*N*-oxide even after 14 days' treatment (table 5), suggesting that the renal function was not impaired as to cause the changes of urinary metabolites, although histological changes was observed.

The change of urinary metabolites by cyclosporine A can be explained as follows. One of the mechanisms of cyclosporine A-induced cholestasis appears to involve inhibition by cyclosporine A of bile acid : CoA ligase activity due to binding at the bile acid binding site [44] and reduction

© 2009 The Authors
Journal compilation © 2009 Nordic Pharmacological Society.

of production of bile acid conjugates [45]. Bile acids are cytotoxic, but when conjugated become less toxic, and in conjugated form are more amenable to renal excretion. Due to inhibition of formation of conjugated bile acids by cyclosporine A, hepatic uptake and biliary excretion of bile acids will be decreased. Therefore, plasma total bile acids were thought to have increased and excretion of bile acids in urine to have decreased in cyclosporine A-treated rats.

Although the mechanisms responsible for the decreases in urinary leucine, isoleucine, valine, and methyl malonate have yet to be clarified in detail, some reports have suggested relationships between liver diseases and changes in branched-chain amino acids (leucine, isoleucine, and valine). Children with mild-moderate chronic cholestatic liver disease had decreased plasma concentrations of branched-chain amino acids in the presence of increased requirements for total branched-chain amino acids [46,47], suggesting that decreases in plasma branched-chain amino acids levels may be reflective of increases in branched-chain amino acids requirements. Correspondingly, urinary branched-chain amino acids levels are considered to be decreased. There is evidence in animal models of liver disease for increased activity of the branched chain keto-acid dehydrogenase complex in liver, suggesting that increased oxidation of the branched-chain amino acids may occur [48].

The magnitudes of area intensities of proton signals derived from 0.66 to 1.90 ppm appear to be altered differently by intra-hepatic and extra-hepatic cholestatic injury caused by cyclosporine A and, 4,4′-methylene dianiline, α-naphthylisothiocyanate or bile duct ligation, respectively, and are thus likely to be useful as biomarkers in urine. We conclude that a bunch of bile acids, valine, and methyl malonate have a possibility to be biomarkers of cholestasis distinguishing a difference in mechanism of toxicity when analysed with data serum bilirubin. ^{1}H nuclear magnetic resonance metabonomics technology appears to be very useful as a means of detecting cholestatic liver injury. Other compounds, like nephrotoxic ones, are also shown to increase amino acids (alanine, isoleucine, leucine, valine) in urine by ^{1}H nuclear magnetic resonance analysis [10,41,42]. Therefore, further studies should be directed toward assessing the endogenous metabolites which can be used as biomarkers to differentiate cholestatic injury from other diseases.

^{1}H nuclear magnetic resonance-based metabonomics can be used to address a large range of preclinical and clinical problems. This study has established the importance of metabonomics technology in examination of the mechanistic complexity of drug toxicity as well as the benefits of this approach in drug safety evaluation and biomarker discovery for drug development.

Acknowledgement

The authors would like to thank all those involved in the performance of this study at Tsukuba Research and Kawashima Research, Drug Safety Research Laboratories, Eisai, with special thanks to Dr. N. Toritsuka, K. Asai, and T. Imade.

References

1 Kola I, Landis J. Can the pharmaceutical industry reduce attrition rates? Nat Rev Drug Discov 2004;**3**:711–5.
2 Steiner G, Suter L, Boess F, Gasser R, de Vera MC, Albertini S *et al.* Discriminating different classes of toxicants by transcript profiling. Environ Health Perspect 2004;**112**:1236–48.
3 Lewis JH, Zimmerman HJ. Drug- and chemical-induced cholestasis. Clin Liver Dis 1999;**3**:433–64.
4 Trauner M, Meier PJ, Boyer JL. Molecular pathogenesis of cholestasis. N Engl J Med 1998;**339**:1217–27.
5 Chitturi S, Farrell GC. Drug-induced cholestasis. Semin Gastrointest Dis 2001;**12**:113–24.
6 Rodriguez-Garay EA. Cholestasis: human disease and experimental animal models. Ann Hepatol 2003;**2**:150–8.
7 Zollner G, Trauner M. Molecular mechanisms of cholestasis. Wien Med Wochenschr 2006;**156**:380–5.
8 Beckwith-Hall BM, Nicholson JK, Nicholls AW, Foxall PJ, Lindon JC, Connor SC *et al.* Nuclear magnetic resonance spectroscopic and principal components analysis investigations into biochemical effects of three model hepatotoxins. Chem Res Toxicol 1998;**11**:260–72.
9 Holmes E, Nicholls AW, Lindon JC, Ramos S, Spraul M, Neidig P *et al.* Development of a model for classification of toxin-induced lesions using ^{1}H NMR spectroscopy of urine .combined with pattern recognition. NMR Biomed 1998;**11**:235–44.
10 Robertson DG, Reily MD, Sigler RE, Wells DF, Paterson DA, Braden TK. Metabonomics: evaluation of nuclear magnetic resonance (NMR) and pattern recognition technology for rapid in vivo screening of liver and kidney toxicants. Toxicol Sci 2000;**57**:326–37.
11 Coen M, Holmes E, Lindon JC, Nicholson JK. NMR-based metabolic profiling and metabonomic approaches to problems in molecular toxicology. Chem Res Toxicol 2008;**21**:9–27.
12 Ishihara K, Katsutani N, Aoki T. A metabonomics study of the hepatotoxicants galactosamine, methylene dianiline and clofibrate in rats. Basic Clin Pharmacol Toxicol 2006;**99**:251–60.
13 Kanz MF, Gunasena GH, Kaphalia L, Hammond DK, Syed YA. A minimally toxic dose of methylene dianiline injures biliary epithelial cells in rats. Toxicol Appl Pharmacol 1998;**150**:414–26.
14 Stone BG, Udani M, Sanghvi A, Warty V, Plocki K, Bedetti CD *et al.* Cyclosporin A-induced cholestasis. Gastroenterology 1987;**93**:344–51.
15 Deters M, Klabunde T, Kirchner G, Resch K, Kaever V. Sirolimus/cyclosporine/tacrolimus interactions on bile flow and biliary excretion of immunosuppressants in a subchronic bile fistula rat model. Br J Pharmacol 2002;**136**:604–12.
16 Galan AI, Fernandez E, Moran D, Munoz ME, Jimenez R. Cyclosporine A hepatotoxicity: effect of prolonged treatment with cyclosporine on biliary lipid secretion in the rat. Clin Exp Pharmacol Physiol 1995;**22**:260–5.
17 McCarthy DJ, Struck RF, Shih TW, Suling WJ, Hill DL, Enke SE. Disposition and metabolism of the carcinogen reduced Michler's ketone in rats. Cancer Res 1982;**42**:3475–9.
18 Lenz EM, Bright J, Knight R, Wilson ID, Major H. Cyclosporin A-induced changes in endogenous metabolites in rat urine: a metabonomic investigation using high field ^{1}H NMR spectroscopy, HPLC-TOF/MS and chemometrics. J Pharm Biomed Anal 2004;**35**:599–608.
19 Weljie AM, Newton J, Mercier P, Carlson E, Slupsky CM. Targeted profiling: quantitative analysis of ^{1}H NMR metabolomics data. Anal Chem 2006;**78**:4430–42.
20 Saude EJ, Slupsky CM, Sykes BD. Optimization of NMR analysis of biological fluids for quantitative accuracy. Metabolomics 2006;**2**:113–23.

© 2009 The Authors
Journal compilation © 2009 Nordic Pharmacological Society.

21 Saude EJ, Sykes BD. Urine stability for metabolomic studies: effects of preparation and storage. Metabolomics 2007;**3**:19–27.
22 Schnackenberg LK, Dragan YP, Reilly MD, Robertson DG, Beger RD. Evaluation of NMR spectral data of urine in conjunction with measured clinical chemistry and histopathology parameters to assess the effects of liver and kidney toxicants. Metabolomics 2007;**3**:87–100.
23 Shearer J, Duggan G, Weljie A, Hittel DS, Wasserman DH, Vogel HJ. Metabolomic profiling of dietary-induced insulin resistance in the high fat-fed C57BL/6J mouse. Diabetes Obes Metab 2008;**10**:950–8.
24 Nicholson JK, Wilson ID. High resolution proton magnetic resonance spectroscopy of biological fluids. Prog Nuclear Magn Reson Spectrosc 1989;**21**:449–501.
25 Lindon JC, Nicholson JK, Everett JR. NMR spectroscopy of biofluids. Ann Rep NMR Spectrosc 1999;**38**:1–88.
26 Ijare OB, Somashekar BS, Gowda GA, Sharma A, Kapoor VK, Khetrapal CL. Quantification of glycine and taurine conjugated bile acids in human bile using ^{1}H NMR spectroscopy. Magn Reson Med 2005;**53**:1441–6.
27 Kanz MF, Kaphalia L, Kaphalia BS, Romagnoli E, Ansari GA. Methylene dianiline: acute toxicity and effects on biliary function. Toxicol Appl Pharmacol 1992;**117**:88–97.
28 Jean PA, Roth RA. Naphthylisothiocyanate disposition in bile and its relationship to liver glutathione and toxicity. Biochem Pharmacol 1995;**50**:1469–74.
29 Kanz MF, Dugas TR, Liu H, Santa Cruz V. Glutathione depletion exacerbates methylenedianiline toxicity to biliary epithelial cells and hepatocytes in rats. Toxicol Sci 2003;**74**:447–56.
30 Waters NJ, Holmes E, Williams A, Waterfield CJ, Farrant RD, Nicholson JK. NMR and pattern recognition studies on the time-related metabolic effects of α-naphthylisothiocyanate on liver, urine, and plasma in the rat: an integrative metabonomic approach. Chem Res Toxicol 2001;**14**:1401–12.
31 Schoonen WG, Kloks CP, Ploemen JP, Smit MJ, Zandberg P, Horbach GJ *et al.* Uniform procedure of ^{1}H NMR analysis of rat urine and toxicometabonomics Part II: comparison of NMR profiles for classification of hepatotoxicity. Toxicol Sci 2007;**98**:286–97.
32 Wang GF, Stacey NH. Elevation of individual serum bile acids on exposure to trichloroethylene or α-naphthylisothiocyanate. Toxicol Appl Pharmacol 1990;**105**:209–15.
33 Kinugasa T, Uchida K, Kadowaki M, Takase H, Nomura Y, Saito Y. Effect of bile duct ligation on bile acid metabolism in rats. J Lipid Res 1981;**22**:201–7.
34 Takada Y, Sano N, Takikawa H. Urinary excretion of bile acids in bile duct-ligated rats. J Gastroenterol 2003;**38**:561–6.
35 Stacey NH, Kotecka B. Inhibition of taurocholate and ouabain transport in isolated rat hepatocytes by cyclosporin A. Gastroenterology 1988;**95**:780–6.
36 Bohme M, Jedlitschky G, Leier I, Buchler M, Keppler D. ATP-dependent export pumps and their inhibition by cyclosporins. Adv Enzyme Regul 1994;**34**:371–80.
37 Farthing MJ, Clark ML. Nature of the toxicity of cyclosporin A in the rat. Biochem Pharmacol 1981;**30**:3311–6.
38 Jackson NM, Hsu CH, Visscher GE, Venkatachalam MA, Humes HD. Alterations in renal structure and function in a rat model of cyclosporine nephrotoxicity. J Pharmacol Exp Ther 1987;**242**:749–56.
39 Gartland KP, Bonner FW, Nicholson JK. Investigations into the biochemical effects of region-specific nephrotoxins. Mol Pharmacol 1989;**35**:242–50.
40 Bairaktari E, Katopodis K, Siamopoulos KC, Tsolas O. Paraquat-induced renal injury studied by ^{1}H nuclear magnetic resonance spectroscopy of urine. Clin Chem 1998;**44**:1256–61.
41 Shockcor JP, Holmes E. Metabonomic applications in toxicity screening and disease diagnosis. Curr Top Med Chem 2002;**2**:35–51.
42 Gibbs A. Comparison of the specificity and sensitivity of traditional methods for assessment of nephrotoxicity in the rat with metabonomic and proteomic methodologies. J Appl Toxicol 2005;**25**:277–95.
43 Waters NJ, Waterfield CJ, Farrant RD, Holmes E, Nicholson JK. Metabonomic deconvolution of embedded toxicity: application to thioacetamide hepato- and nephrotoxicity. Chem Res Toxicol 2005;**18**:639–54.
44 Vessey DA, Kelley M. Inhibition of bile acid conjugation by cyclosporin A. Biochim Biophys Acta 1995;**1272**:49–52.
45 Moran D, De Buitrago JM, Fernandez E, Galan AI, Munoz ME, Jimenez R. Inhibition of biliary glutathione secretion by cyclosporine A in the rat: possible mechanisms and role in the cholestasis induced by the drug. J Hepatol 1998;**29**:68–77.
46 Chin SE, Shepherd RW, Thomas BJ, Cleghorn GJ, Patrick MK, Wilcox JA *et al.* Nutritional support in children with end-stage liver disease: a randomized crossover trial of a branched-chain amino acid supplement. Am J Clin Nutr 1992;**56**:158–63.
47 Mager DR, Wykes LJ, Roberts EA, Ball RO, Pencharz PB. Branched-chain amino acid needs in children with mild-to-moderate chronic cholestatic liver disease. J Nutr 2006;**136**:133–9.
48 Honda T, Fukuda Y, Nakano I, Katano Y, Goto H, Nagasaki M *et al.* Effects of liver failure on branched-chain α-keto acid dehydrogenase complex in rat liver and muscle: comparison between acute and chronic liver failure. J Hepatol 2004;**40**:439–45.

© *2009 The Authors*
Journal compilation © 2009 Nordic Pharmacological Society.

0090-9556/09/3707-1513–1520$20.00
DRUG METABOLISM AND DISPOSITION
Copyright © 2009 by The American Society for Pharmacology and Experimental Therapeutics
DMD 37:1513–1520, 2009

Vol. 37, No. 7
26567/3478493
Printed in U.S.A.

DMD

DRUG METABOLISM AND DISPOSITION

aspet

Human Arylacetamide Deacetylase Is a Principal Enzyme in Flutamide Hydrolysis

Akinobu Watanabe, Tatsuki Fukami, Miki Nakajima, Masataka Takamiya, Yasuhiro Aoki, and Tsuyoshi Yokoi

Drug Metabolism and Toxicology, Faculty of Pharmaceutical Sciences, Kanazawa University, Kakuma-machi, Kanazawa, Japan (A.W., T.F., M.N., T.Y.); and Department of Legal Medicine, Iwate Medical University School of Medicine, Uchimaru, Morioka, Japan (M.T., Y.A.)

Received January 19, 2009; accepted March 26, 2009

ABSTRACT:

Flutamide, an antiandrogen drug, is widely used for the treatment of prostate cancer. The initial metabolic pathways of flutamide are hydroxylation and hydrolysis. It was recently reported that the hydrolyzed product, 4-nitro-3-(trifluoromethyl)phenylamine (FLU-1), is further metabolized to *N*-hydroxy FLU-1, an assumed hepatotoxicant. However, the esterase responsible for the flutamide hydrolysis has not been characterized. In the present study, we found that human arylacetamide deacetylase (AADAC) efficiently hydrolyzed flutamide using recombinant AADAC expressed in COS7 cells. In contrast, carboxylesterase1 (CES1) and CES2, which are responsible for the hydrolysis of many drugs, could not hydrolyze flutamide. AADAC is specifically expressed in the endoplasmic reticulum. Flutamide hydrolase activity was highly detected in human liver microsomes (K_m, 794 ± 83 μM; V_{max}, 1.1 ± 0.0 nmol/min/mg protein), whereas the activity was extremely low in human liver cytosol. The flutamide hydrolase activity in human liver microsomes was strongly inhibited by bis-(nonylphenyl)-phenylphosphate, diisopropylphosphorofluoride, and physostigmine sulfate (eserine) but moderately inhibited by sodium fluoride, phenylmethylsulfonyl fluoride, and disulfiram. The same inhibition pattern was obtained with the recombinant AADAC. Moreover, human liver and jejunum microsomes showing AADAC expression could hydrolyze flutamide, but human pulmonary and renal microsomes, which do not express AADAC, showed slight activity. In human liver microsomal samples (n = 50), the flutamide hydrolase activities were significantly correlated with the expression levels of AADAC protein (r = 0.66, p < 0.001). In conclusion, these results clearly showed that flutamide is exclusively hydrolyzed by AADAC. AADAC would be an important enzyme responsible for flutamide-induced hepatotoxicity.

Flutamide (3′-trifluoro-2-methyl-4′-nitro-2-methyl-propinoylanilide) is a nonsteroidal antiandrogen drug used for the treatment of prostate cancer. The combination of luteinizing hormone-releasing hormone agonist results in prolonged survival in prostate cancer patients (Crawford et al., 1989). However, flutamide occasionally causes severe hepatotoxicity (Thole et al., 2004). Flutamide itself is not toxic when used at the appropriate clinical dose, but bioactivation of flutamide has been considered to be the cause of flutamide-induced hepatotoxicity (Fau et al., 1994).

Flutamide is mainly metabolized to 2-hydroxyflutamide by human CYP1A2. It has been suggested that 2-hydroxyflutamide is associated with the therapeutic effect of flutamide (Katchen and Buxbaum, 1975). Flutamide is also hydrolyzed to 4-nitro-3-(trifluoromethyl)phenylamine (FLU-1) by esterase (Katchen and Buxbaum, 1975; Schulz et al., 1988). FLU-1 is considered to have no therapeutic effect (Aizawa et al., 2003). Goda et al. (2006) recently reported that FLU-1 is further metabolized to *N*-hydroxyl FLU-1 by human CYP3A4. Many researchers have reported on the relationship between the toxicity and metabolism of flutamide. It was shown in CYP1A2 knockout SV129 mice but not in wild-type mice that the urinary concentration of FLU-1 was increased, and an abnormal elevation of alanine aminotransferase was shown after the knockout mice were fed an amino acid-deficient diet (Matsuzaki et al., 2006). It was also shown in humans that the urinary caffeine metabolite ratio, an indicator of the CYP1A2 activity, was significantly lower in patients with hepatic injury compared with patients with normal hepatic function after the same flutamide therapy (Ozono et al., 2002). In addition, a study on patients of prostate cancer taking flutamide showed that the incidence of hepatotoxicity was correlated with the plasma concentration of FLU-1 (Aizawa et al., 2003). More recently, Ohbuchi et al. (2009) reported that coadministration of FLU-1 and 1,4-bis[2-(3,5-dichloropyridyloxy)]benzene, an inducer of CYP3A and CYP1A, to mice significantly increased serum alanine aminotransferase, and sev-

Article, publication date, and citation information can be found at http://dmd.aspetjournals.org.
doi:10.1124/dmd.109.026567.

ABBREVIATIONS: FLU-1, 4-nitro-3-(trifluoromethyl)phenylamine; CES, carboxylesterase; HLM, human liver microsome; BNPP, bis-(nonylphenyl)-phenylphosphate; AADAC, arylacetamide deacetylase; DFP, diisopropylphosphorofluoride; eserine, physostigmine sulfate; PMSF, phenylmethylsulfonyl fluoride; $AgNO_3$, silver nitrate; $CdCl_2$, cadmium chloride; $CoCl_2$, cobaltous chloride; $CuCl_2$, cupric chloride; PNPA, *p*-nitrophenyl acetate; NaF, sodium fluoride; HLC, human liver cytosol; HJM, human jejunum microsome; HPM, human pulmonary microsome; HRM, human renal microsome; RT-PCR, reverse transcription-polymerase chain reaction; GAPDH, glyceraldehyde 3-phosphate dehydrogenase; SNP, single nucleotide polymorphism; DMSO, dimethyl sulfoxide; HPLC, high-performance liquid chromatography.

Downloaded from dmd.aspetjournals.org at Kanazawa Univ Yakugakubu Lib on September 22, 2009

DMD DRUG METABOLISM AND DISPOSITION aspet

eral protein adducts were detected after incubation of the microsomal protein with *N*-hydroxy FLU-1. Therefore, the hepatotoxicity of flutamide might be related to *N*-hydroxy FLU-1. Considering these reports, the hydrolysis pathway may contribute to the hepatotoxicity of flutamide.

Carboxylesterase (CES) is the major serine esterase contributing to the hydrolysis of various drugs and xenobiotics. In human, CES isoforms are classified into three families: CES1, CES2, and CES3. CES1 and CES2 have been reported to be responsible for the biotransformation of a number of clinically used drugs and prodrugs such as imidapril, capecitabine, and irinotecan (Imai et al., 2006). CES3 appears to show extremely low activity compared with CES1 and CES2 (Sanghani et al., 2004). The flutamide hydrolysis by human liver microsomes (HLM) is inhibited by bis-(nonylphenyl)-phenylphosphate (BNPP), a general CES inhibitor (Heymann and Krisch, 1967; Block and Arndt, 1978; Mentlein et al., 1988). Thus, it is plausible that flutamide is hydrolyzed by CES. However, the flutamide hydrolase activity was not detected by using purified CES1 (pI 4.5) and CES2 (pI 5.3) (Takai et al., 1997). Therefore, we considered that another esterase expressed in HLM plays a role in flutamide hydrolysis. As a candidate enzyme, arylacetamide deacetylase (AADAC) could be considered.

AADAC, as well as CES1 and CES2, is a major serine hydrolase expressed in HLM (Ross and Crow, 2007). AADAC was first identified as the enzyme that catalyzes the deacetylation of 2-acetylaminofluorene (Probst et al., 1991). The active site domain of AADAC shares high homology with that of hormone-sensitive lipase (Probst et al., 1994). Therefore, AADAC has been classified as a lipase. In fact, Tiwari et al. (2007) proved that human AADAC was capable of hydrolyzing cholesterol ester when expressed in yeast. However, it is unknown whether AADAC is involved in the hydrolysis of clinical therapeutic drugs. In the present study, the involvement of human AADAC in flutamide hydrolysis was investigated.

Materials and Methods

Chemicals and Reagents. Flutamide, 4-nitro-3-(trifluoromethyl)phenylamine (FLU-1), *p*-nitrophenol, diisopropylphosphorofluoride (DFP), physostigmine sulfate (eserine), phenylmethylsulfonyl fluoride (PMSF), disulfiram, silver nitrate ($AgNO_3$), cadmium chloride ($CdCl_2$), cobaltous chloride ($CoCl_2$), and cupric chloride ($CuCl_2$) were purchased from Wako Pure Chemical Industries (Osaka, Japan). *p*-Nitrophenyl acetate (PNPA), BNPP, and sodium fluoride (NaF) were purchased from Sigma-Aldrich (St. Louis, MO). Primers were commercially synthesized at Hokkaido System Sciences (Sapporo, Japan). The random hexamer and SYBR Premix Ex Taq were from Takara (Shiga, Japan). RevaTra Ace (Moloney murine leukemia virus reverse transcriptase RNase H−) was obtained from Toyobo (Tokyo, Japan). All the other chemicals used in this study were of analytical or the highest quality commercially available.

Human Tissues. The microsomes or cytosol from human liver, jejunum, lung, and kidney were used in this study. Pooled HLM (n = 50), individual HLM (24 donors), and pooled human liver cytosol (HLC, n = 22) were purchased from BD Gentest (Woburn, MA). Individual HLM from 15 donors were also obtained from Human and Animal Bridging Research Organization (Chiba, Japan), and those from 11 donors were obtained from autopsy materials that were discarded after pathological investigation. Human jejunum microsomes (HJM, pooled, n = 10), human pulmonary microsomes (HPM, single donor), and human renal microsomes (HRM, single donor) were purchased from Tissue Transformation Technologies (Edison, NJ). The pooled HLM, HJM, HPM, and HRM were used for the immunoblotting analysis and the assay of flutamide hydrolase activity. The HLC was used for the comparison of flutamide hydrolase activity with HLM. The individual HLM samples were used for the correlation analysis. The use of the human tissues was approved by the Ethics Committees of Kanazawa University (Kanazawa, Japan) and Iwate Medical University (Morioka, Japan).

TABLE 1

Primers used in the present study

Primer	Sequence
For detection of real-time RT-PCR	
AADAC-RT-S	5′-TTGTGGAGCTCCTGGGACTT-3′
AADAC-RT-AS	5′-TCTGTCTGCTGTCCATCTTG-3′
For construction of expression plasmids	
AADAC-S	5′-TAGAGACCAAGAAGCGGGAC-3′
AADAC-AS	5′-GCTACATGTTTTACTATAGATTTTCC-3′
CES1A1-S	5′-AGAGACCTCGCAGGCCCCGA-3′
CES1A2-S	5′-GAGACCTCGCAGGCCCCCG-3′
CES1A-AS	5′-CCATGGTAAGATGCCTTCTG-3′
CES2A1-S	5′-CCTGCCTACCACTAGATCCC-3′
CES2A1-AS	5′-CTCGCCTGTCAGCGAACCCAC-3′

Total RNA from Human Tissues and Reverse Transcription-Polymerase Chain Reaction Analyses. Total RNA samples from normal human liver (single donor), colon (pooled, n = 2), kidney (single donor), bladder (pooled, n = 2), breast (pooled, n = 2), ovary (single donor), and uterus (pooled, n = 3) were obtained from Stratagene (La Jolla, CA). Total RNA samples from normal human lung (single donor) and testis (single donor) were from Cell Applications (San Diego, CA). Total RNA samples from normal human stomach (single donor), adrenal gland (pooled, n = 62), and small intestine (pooled, n = 5) were from Clontech (Palo Alto, CA). The reverse transcription procedure was described previously (Nakajima et al., 2006).

For quantitative analysis, real-time reverse transcription-polymerase chain reaction (RT-PCR) was performed for AADAC mRNA using an MX3000P real-time PCR system (Stratagene). The forward and reverse primers used for PCR were AADAC-RT-S and AADAC-RT-AS primers (Table 1). A 1-μl portion of the reverse-transcribed mixture was added to a PCR mixture containing 10 pmol of each primer and 12.5 μl of SYBR Premix Ex Taq solution in a final volume of 25 μl. After an initial denaturation at 95°C for 30 s, the amplification was performed by denaturation at 94°C for 4 s, annealing at 58°C for 7 s, and extension at 72°C for 20 s for 45 cycles. Human glyceraldehyde 3-phosphate dehydrogenase (GAPDH) mRNA was also quantified according to a method described previously (Tsuchiya et al., 2004). The copy numbers were calculated using standard amplification curves.

Construction of Plasmids Expressing Human AADAC, CES1A, and CES2. The full-length human AADAC, CES1A1, CES1A2, and CES2A1 cDNAs were obtained by RT-PCR using a human liver RNA sample as the initial template. The primers used are shown in Table 1. In this study, two clones of AADAC cDNA were obtained [c.931guanine (G) and adenine (A)]. In the reference sequence of NM 001086.2, the nucleotide at the c.931 position is G. Therefore, the clones with c.931G and c.931A were defined as the AADAC wild-type and AADAC variant, respectively. This single nucleotide polymorphism (SNP, c.931G>A) leads to an amino acid change of valine to isoleucine. The allele frequency of this SNP (ID: rs1803155) has been reported to be approximately 55 to 80% in each population, including European, Asian, and sub-Saharan African in the dbSNP database in the National Center for Biotechnology Information (http://www.ncbi.nlm.nih.gov/SNP/snp_ref.cgi?rs = 1803155). The PCR products were subcloned into pTARGET mammalian expression vector (Promega, Madison, WI). The nucleotide sequences were confirmed by DNA sequence analysis (Long-Read Tower DNA sequencer; GE Healthcare, Little Chalfont, Buckinghamshire, UK).

Transfection of Plasmids Expressing Human AADAC, CES1A, and CES2. African green monkey kidney cells, COS7 cells, were obtained from American Type Culture Collection (Manassas, VA). The COS7 cells were grown in Dulbecco's modified Eagle's medium containing 4.5 g/l glucose and 10% fetal bovine serum with 5% CO_2 at 37°C. The cells were transfected in 10-cm dishes with 7.5 μg of each expression plasmid using Lipofectamine (Invitrogen, Carlsbad, CA). After incubation for 48 h, the cells were harvested and suspended in a small amount of TGE buffer (10 mM Tris-HCl, 20% glycerol, 1 mM EDTA, pH 7.4) and disrupted by freeze-thawing three times. Each protein expression level was determined by immunoblot analysis as described below.

Downloaded from dmd.aspetjournals.org at Kanazawa Univ Yakugakubu Lib on September 22, 2009

DMD DRUG METABOLISM AND DISPOSITION aspet

Immunoblot Analysis. SDS-polyacrylamide gel electrophoresis and immunoblot analysis were performed according to Laemmli (1970). Enzyme sources (30 μg) were separated on 10% polyacrylamide gels and electrotransferred onto polyvinylidene difluoride membrane, Immobilon-P (Millipore Corporation, Billerica, MA). The membranes were probed with monoclonal mouse anti-human AADAC (Abnova, Neihu District, Taipei City, Taiwan), polyclonal rabbit anti-human CES1 (Abcam, Cambridge, MA), and polyclonal rabbit anti-human CES2 antibodies (Antagene, San Francisco, CA), and the corresponding fluorescent dye-conjugated second antibody and an Odyssey infrared imaging system (LI-COR Biosciences, Lincoln, NE) were used for the detection. The relative expression level was quantified using ImageQuant TL Image Analysis software (GE Healthcare).

Flutamide Hydrolase Activity. The flutamide hydrolase activity was determined as follows: a typical incubation mixture (final volume of 0.2 ml) contained 100 mM potassium phosphate buffer, pH 7.4, and various enzyme sources (human microsomal protein and COS7 cell homogenate expressing esterases, 0.4 mg/ml; human cytosolic protein, 1.0 mg/ml). In the preliminary study, we confirmed that the rate of formation of FLU-1 was linear with respect to the protein concentrations (<1.0 mg/ml human microsomal protein and COS7 cells homogenate expressing esterases and <1.5 mg/ml human cytosolic protein) and incubation time (<60 min). Flutamide was dissolved in dimethyl sulfoxide (DMSO), and the final concentration of DMSO in the incubation mixture was 1.0%. The reaction was initiated by the addition of 25 to 750 μM flutamide after 2-min preincubation at 37°C. After the 30-min incubation at 37°C, the reaction was terminated by the addition of 0.1 ml of ice-cold acetonitrile. After removal of the protein by centrifugation at 9500*g* for 5 min, a 60-μl portion of the supernatant was subjected to high-performance liquid chromatography (HPLC). The HPLC analysis was performed using an L-7100 pump (Hitachi, Tokyo, Japan), an L-7200 autosampler (Hitachi), an L-7405 UV detector (Hitachi), and a D-2500 Chromato-Integrator (Hitachi) equipped with a Mightysil RP-18 C18 GP column (5-μm particle size, 4.6 mm i.d.×150 mm; Kanto Chemical, Tokyo, Japan). The eluent was monitored at 376 nm with a noise-base clean Uni-3 (Union, Gunma, Japan), which can reduce the noise by integrating the output and increase the signal 3-fold by differentiating the output, and 5-fold by further amplification with an internal amplifier, resulting in a maximum 15-fold amplification of the signal. The mobile phase was 45% acetonitrile containing 25 mM ammonium acetate, pH 5.0. The flow rate was 1.0 ml/min. The column temperature was 35°C. The quantification of FLU-1 was performed by comparing the HPLC peak height with that of an authentic standard. Because FLU-1 contaminants exist in the commercially available flutamide to the extent of ~0.5%, the content of FLU-1 in the mixture incubated without the enzyme was subtracted from that with the enzyme to correct the activity. The activity in each concentration was determined as the mean value in triplicate. For kinetic analyses of flutamide hydrolase activity, the parameters were estimated from the fitted curves using a computer program (KaleidaGraph, Synergy Software, Reading, PA) designed for nonlinear regression analysis.

To clarify the involvement of various esterases, inhibition analysis of flutamide hydrolysis was performed by using representative esterase inhibitors. Organophosphates such as BNPP and DFP are known as general CES inhibitors (Heymann and Krisch, 1967; Yamaori et al., 2006). Eserine and NaF are cholinesterase inhibitors (Iwatsubo, 1965; Preuss and Svensson, 1996). EDTA is a paraoxonase inhibitor (Gonzalvo et al., 1997). PMSF is a serine hydrolase inhibitor (Johnson and Moore, 2000). Because heavy metals are frequently used for esterase inhibition studies, $AgNO_3$, $CdCl_2$, $CoCl_2$, and $CuCl_2$ were also used as inhibitors. Disulfiram was reported as a monoacylglycerol lipase inhibitor (Labar et al., 2007). The concentration of BNPP and DFP ranged from 0.001 to 1 mM, and that of the others was 0.1 and 1 mM. PMSF and disulfiram were dissolved in DMSO such that the final concentration of DMSO in the incubation mixture was 1.5%. Other inhibitors were dissolved in distilled water. The experimental procedure and condition were the same as above except that 500 μM flutamide was added. It was confirmed that 1.5% DMSO did not inhibit the flutamide hydrolase activity, and the control activity was determined in the presence of 1.5% DMSO.

***p*-Nitrophenyl Acetate Hydrolase Activity.** To confirm whether the recombinant AADAC, CES1, and CES2 are enzymatically active, the PNPA, a general esterase substrate, hydrolase activity was measured. The PNPA hydrolase activity was determined as follows: a typical incubation mixture was the same as above. PNPA was dissolved in DMSO, and the final concentration of DMSO in the incubation mixture was 1.0%. The reaction was initiated by the addition of 500 μM PNPA after 2-min preincubation at 37°C. After 5-min incubation at 37°C, the reaction was terminated by the addition of 0.1 ml of ice-cold methanol. The PNPA hydrolase activity was measured by the absorbance at 405 nm using Biotrak II plate reader (GE Healthcare). The quantification of *p*-nitrophenol, a metabolite of PNPA hydrolysis, was performed by comparing the absorbance with that of an authentic standard. Because *p*-nitrophenol contaminants exist in the commercially available PNPA to the extent of ~5%, the content of *p*-nitrophenol in the mixture incubated without the enzyme was subtracted from that with the enzyme to correct the activity.

Statistical Analysis. Comparison of two groups was made with unpaired, two-tailed Student's *t* test. Correlation analyses were performed by Spearman rank method. A value of $p < 0.05$ was considered statistically significant.

Results

PNPA and Flutamide Hydrolase Activities by Recombinant Human AADAC Wild-Type, AADAC Variant, CES1A1, CES1A2, and CES2. To compare the flutamide hydrolase activity between human AADAC, CES1A1, CES1A2, and CES2, they were transiently expressed in COS7 cells. The AADAC variant was also transiently expressed in COS7 cells. The protein expression levels were determined by immunoblot analysis (Fig. 1A). AADAC protein was specifically expressed in COS7 cells transfected with the expression plasmids of AADAC wild-type and variant. CES1A and CES2 proteins were specifically expressed in COS7 cells transfected with the expression plasmids of CES1A1 or CES1A2, and CES2, respectively. To confirm that these enzymes were enzymatically active, PNPA hydrolase activity was measured at a concentration of 500 μM PNPA (Fig. 1B). The recombinant CES2A1 showed the highest PNPA hydrolase activity (621 ± 61 nmol/min/mg protein), and the recombinant AADAC wild-type, variant, CES1A1, and CES1A2 showed similar activities (243 ± 11, 247 ± 24, 293 ± 19, and 245 ± 18 nmol/min/mg protein, respectively). The flutamide hydrolase activities were determined at a concentration of 500 μM flutamide (Fig. 1C). Among them, the AADAC wild-type and variant showed flutamide hydrolase activity (0.28 ± 0.03 and 0.30 ± 0.01 nmol/min/mg protein, respectively). In contrast, CES1A1, CES1A2, and CES2 showed almost no activity (0.003 ± 0.003, 0.008 ± 0.008, and 0.012 ± 0.007 nmol/min/mg protein, respectively), similar to mock COS7 cells (0.012 ± 0.007 nmol/min/mg protein). These results suggested that AADAC, but not the CES enzymes, contributed to the flutamide hydrolysis.

Kinetic Analyses of Flutamide Hydrolase Activity by HLM, HLC, and Recombinant Human AADAC. It was previously suggested that AADAC is localized to the endoplasmic reticulum lumen (Frick et al., 2004). Therefore, it is assumed that flutamide can be hydrolyzed in HLM rather than in HLC. In this study, the flutamide hydrolase activity in HLM and HLC was measured (Fig. 2A). The maximum concentration was 750 μM because of the limited solubility of flutamide in the incubation mixture. For HLM, the K_m and V_{max} values were 794 ± 83 μM and 1.1 ± 0.0 nmol/min/mg protein, respectively, resulting in an intrinsic clearance of 1.4 ± 0.1 μl/min/mg protein. For HLC, because the flutamide hydrolase activity ranging from 25 to 750 μM was linear, the K_m and V_{max} values could not be calculated by the Michaelis-Menten equation. The K_m value of the flutamide hydrolase activity by HLC appeared to be substantially higher than that by HLM. These results suggested that the contribution to flutamide hydrolysis by HLM was much higher than that by HLC. In addition, kinetic analyses of the flutamide hydrolase activity by the recombinant AADAC wild-type and variant were also performed (Fig. 2B). The K_m and V_{max} values of the AADAC wild-type were 778 ± 122 μM and 0.6 ± 0.1 nmol/min/mg

Downloaded from dmd.aspetjournals.org at Kanazawa Univ Yakugakubu Lib on September 22, 2009

DMD DRUG METABOLISM AND DISPOSITION aspet

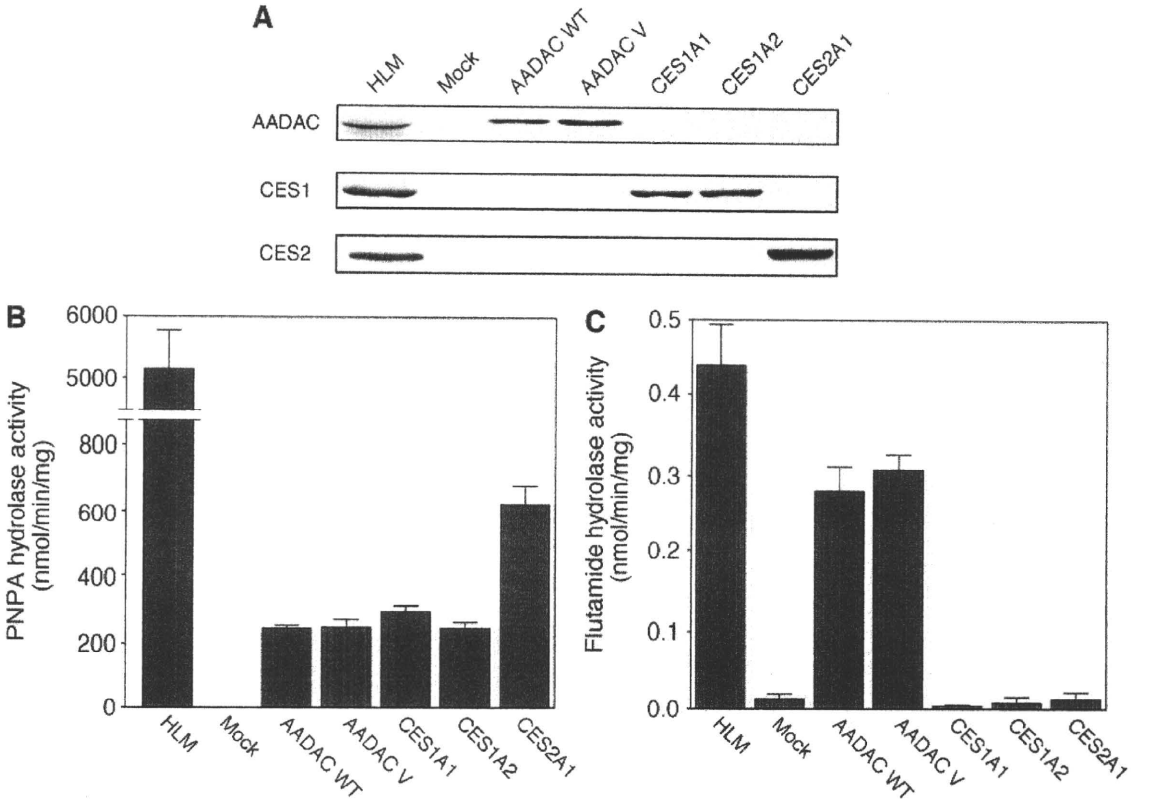

FIG. 1. A, immunoblot analysis of recombinant human AADAC, CES1, and CES2 expressed in COS7 cells. Total cell homogenates from COS7 cells (30 μg) were separated by electrophoresis using 10% SDS-polyacrylamide gel. PNPA hydrolase activities (B) and flutamide hydrolase activities (C) by recombinant AADAC, CES1, and CES2. The homogenates of COS7 cells expressing these enzymes were incubated with 100 μM PNPA or 500 μM flutamide. Each column represents the mean ± S.D. of triplicate determinations. WT, wild type; V, variant.

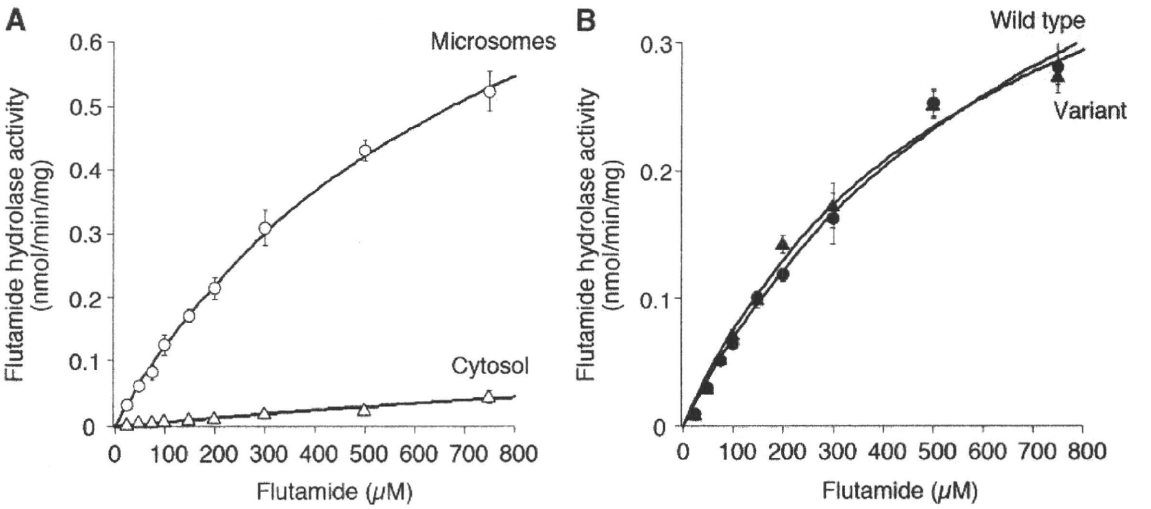

FIG. 2. Kinetic analyses of flutamide hydrolase activities in HLM and HLC (A) and by the recombinant AADAC wild-type and variant (B). The kinetic parameters were estimated from the fitted curve using the computer program KaleidaGraph designed for nonlinear regression analysis. Each data point represents the mean ± S.D. of triplicate determination.

protein, respectively, resulting in an intrinsic clearance of 0.8 ± 0.0 μl/min/mg protein. The K_m and V_{max} values of the AADAC variant were 591 ± 75 μM and 0.5 ± 0.0 nmol/min/mg protein, respectively, resulting in an intrinsic clearance of 0.9 ± 0.1 μl/min/mg protein. Thus, the AADAC variant did not alter the flutamide hydrolase activity. In addition, the K_m values of HLM and AADAC wild-type were not significantly different. These results suggested that AADAC was involved in flutamide hydrolysis in human liver.

Effects of Chemical Inhibitors on Flutamide Hydrolase Activity in HLM and Recombinant AADAC. To prove that AADAC is a principal enzyme for flutamide hydrolysis in human liver, the effects of inhibitors on the flutamide hydrolase activities by HLM and the

Downloaded from dmd.aspetjournals.org at Kanazawa Univ Yakugakubu Lib on September 22, 2009

DRUG METABOLISM AND DISPOSITION DMD aspet

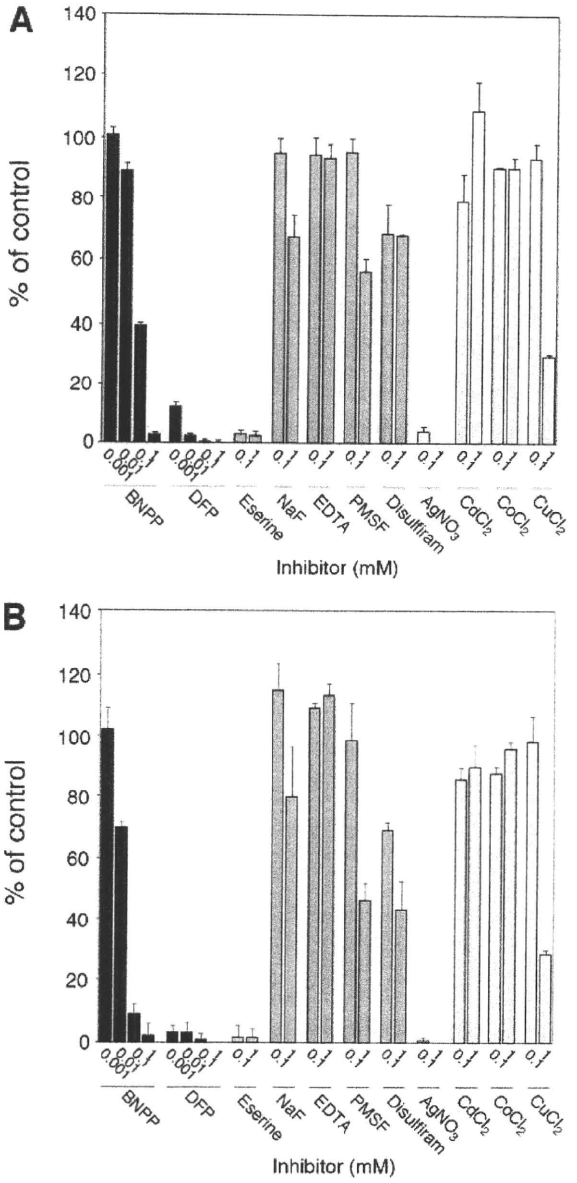

FIG. 3. Effects of chemical inhibitors on flutamide hydrolase activity. Flutamide hydrolase activities in HLM (A) and the recombinant AADAC (B) wild-type were determined at a substrate concentration of 500 μM. The control activity values were 0.438 (A) and 0.283 (B) nmol/min/mg protein, respectively. Each column represents the mean ± S.D. of triplicate determinations.

recombinant AADAC were analyzed. In this study, representative inhibitors of various esterases were used to clarify the involvement of various esterases and examine the inhibitory characteristics of AADAC. The flutamide hydrolase activity by HLM was inhibited in a BNPP concentration-dependent manner and was potently inhibited by 0.01 to 1 mM DFP, 0.1 to 1 mM eserine, and $AgNO_3$ (Fig. 3A). In addition, the flutamide hydrolase activity by HLM was moderately inhibited by 1 mM NaF, PMSF, disulfiram, and $CuCl_2$. However, no inhibition occurred by EDTA, $CaCl_2$, and $CoCl_2$. A similar inhibition pattern was obtained by the recombinant AADAC wild-type (Fig. 3B) and variant (data not shown). These results imply that AADAC is a major esterase responsible for the flutamide hydrolysis in human liver.

Expression of AADAC mRNA in Human Normal Tissues. The expression level of AADAC mRNA in human tissues was determined by

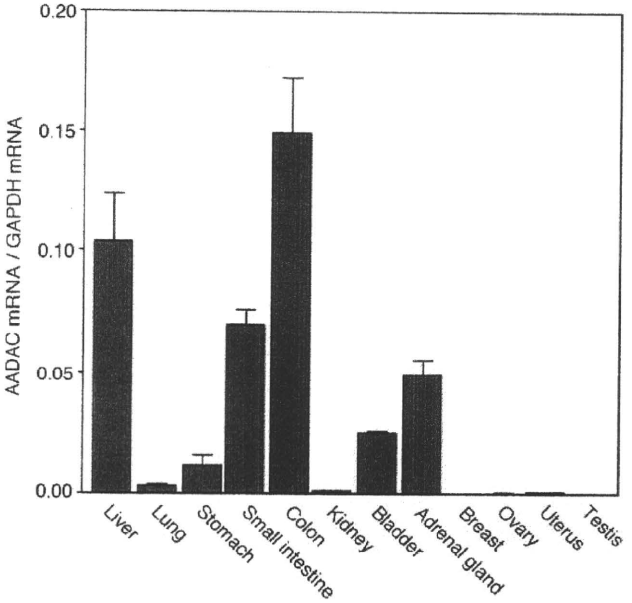

FIG. 4. Expression levels of AADAC mRNA in various human normal tissues. Relative copy numbers of AADAC to GAPDH in human tissues were determined by real-time RT-PCR analysis. Each column represents the mean ± S.D. of triplicate determinations.

real-time RT-PCR analysis (Fig. 4). The expression level of AADAC mRNA was normalized with GAPDH mRNA level. AADAC mRNA is highly expressed in colon, liver, and small intestine and moderately expressed in adrenal gland, bladder, and stomach. Other tissues investigated in this study showed low expression levels. We previously examined the expressions of CES1A1, CES1A2, and CES2 mRNA in human normal tissues (T. Maruichi, M. Katoh, S. Takahashi, M. Nakajima, and T. Yokoi, unpublished data). The expression levels of AADAC mRNA in all the tissues except colon and adrenal gland were lower than those of these CES mRNA. The expression level of AADAC in human liver was 116-, 23-, and 8-fold lower than those of CES1A1, CES1A2, and CES2, respectively.

Expression of AADAC Protein and Flutamide Hydrolase Activities in Human Tissues. To further analyze whether AADAC is responsible for the flutamide hydrolysis in humans, the expression of AADAC and the flutamide hydrolase activity in various human tissues were measured. The expression levels of AADAC, CES1A, and CES2 proteins in HLM, HJM, HPM, and HRM were determined by immunoblot analysis (Fig. 5A). AADAC protein was expressed in HLM and HJM but not in HPM and HRM. This result corresponded with the expression of AADAC mRNA (Fig. 4). CES1A protein was expressed in HLM and HPM, whereas CES2 protein was expressed in HLM, HJM, and HRM. High flutamide hydrolase activity at a concentration of 500 μM flutamide was detected in HJM (0.72 ± 0.02 nmol/min/mg protein) and HLM (0.43 ± 0.03 nmol/min/mg protein). The fact that the hydrolase activity in HJM was higher than that in HLM was supported by the results of the immunoblot analysis. On the other hand, HPM, in which CES1A is expressed, and HRM, in which CES2 is expressed, showed slight hydrolase activity (0.02 ± 0.00 and 0.01 ± 0.01 nmol/min/mg protein, respectively). These results suggested that AADAC is responsible for the flutamide hydrolysis in humans.

Correlation Analysis between Flutamide Hydrolase Activity and AADAC Protein Expression Level. The flutamide hydrolase activities in microsomes from 50 human livers were determined at a concentration of 500 μM. The flutamide hydrolase activities ranged

Downloaded from dmd.aspetjournals.org at Kanazawa Univ Yakugakubu Lib on September 22, 2009

DMD DRUG METABOLISM AND DISPOSITION aspet

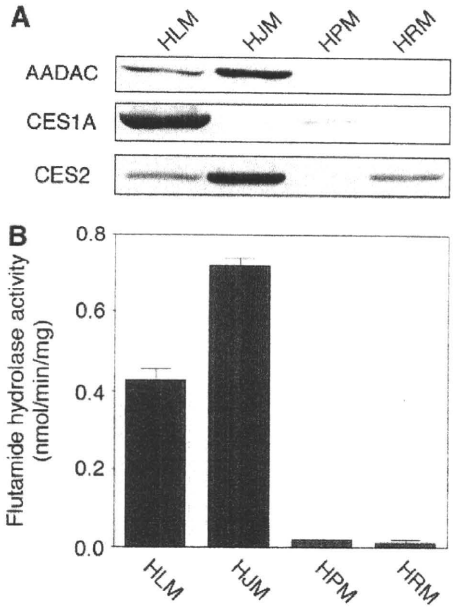

FIG. 5. A, immunoblot analysis of AADAC, CES1A, and CES2 in HLM, HJM, HPM, and HRM. Total cell homogenates from COS7 cells (30 μg) were separated by electrophoresis using 10% SDS-polyacrylamide gel. B, flutamide hydrolase activities in microsomes. The microsomes were incubated with 500 μM flutamide. Each column represents the mean ± S.D. of triplicate determinations.

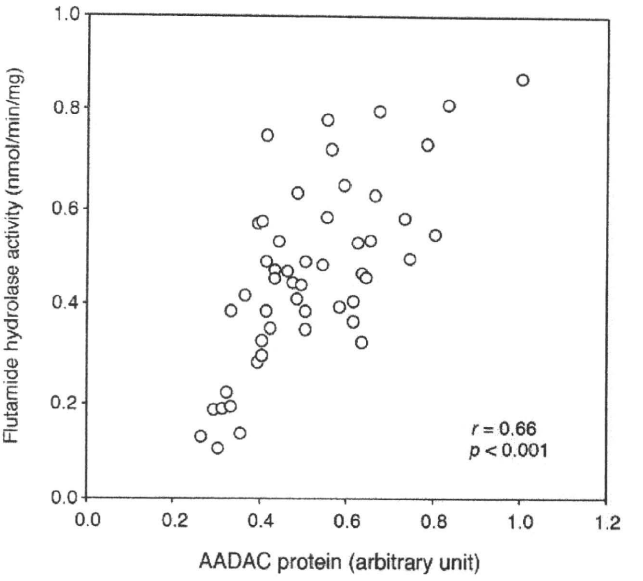

FIG. 6. Correlation between the expression levels of AADAC protein and flutamide hydrolase activities in 50 HLM. The expression level of AADAC protein was determined by immunoblot analysis. The flutamide hydrolase activity was determined by HPLC.

from 0.11 to 0.87 nmol/min/mg protein (mean ± S.D., 0.47 ± 0.19 nmol/min/mg protein), resulting in 7.9-fold interindividual variability. In addition, the expression levels of AADAC protein in microsomes from 50 human livers were determined by immunoblot analysis. The AADAC protein expression levels are represented as relative levels to the sample, which is the highest expression level. The relative expression levels of AADAC protein in HLM ranged from 0.26 to 1.00, resulting in 3.8-fold interindividual variability. As shown in Fig. 6, the expression level of AADAC protein and the flutamide hydrolase activity were significantly correlated ($r = 0.66$, $p < 0.001$). These results also supported that AADAC is a principal enzyme for the flutamide hydrolysis.

Discussion

Human AADAC was first identified as an enzyme that catalyzes the deacetylation of 2-acetylaminofluorene (Probst et al., 1991). It has been believed that AADAC might function as a lipase because of the high homology of the active site of AADAC with that of hormone-sensitive lipase (Probst et al., 1994). On the other hand, human CES enzymes are major serine esterases involved in the hydrolysis of various drugs and xenobiotics. AADAC is one of the major serine esterases expressed in HLM and CES enzymes (Ross and Crow, 2007), but it was unknown whether AADAC is involved in the hydrolysis of therapeutic drugs.

An antiandrogen drug, flutamide, has been widely used for prostate cancer, but severe hepatotoxicity sometimes occurred. Several studies suggested that the flutamide-induced hepatotoxicity was caused by FLU-1, a metabolite of hydrolyzed flutamide, or *N*-hydroxyl FLU-1, a metabolite of FLU-1 by CYP3A or CYP1A (Aizawa et al., 2003; Matsuzaki et al., 2006; Ohbuchi et al., 2009). Therefore, it was considered that flutamide hydrolysis was important in the occurrence of hepatotoxicity, but the flutamide hydrolase enzyme had never been identified. It was conceivable that human CES enzymes CES1A and CES2 are responsible for the hydrolysis of flutamide because they contribute largely to the hydrolysis of various drugs and xenobiotics. However, it was reported that the flutamide hydrolase activity was not detected by using purified CES1A and CES2 (Takai et al., 1997), which is consistent with our finding that the recombinant CES1A1, CES1A2, and CES2A1 did not show the flutamide hydrolase activity (Fig. 1C). Moreover, the activity was scarcely detected in HPM and HRM, in which CES1A and CES2 enzymes were expressed, respectively. On the other hand, the recombinant AADAC showed the flutamide hydrolase activity, and the activity was highly detected in HLM and HJM, in which AADAC is expressed. Furthermore, the similar activities of flutamide hydrolysis in HLM and the recombinant AADAC were consistent with the similar blot densities of AADAC (Fig. 1, A and C). Thus, we found that human AADAC is a major contributor to the flutamide hydrolysis. PNPA hydrolase activity, a general esterase activity, was detected in recombinant AADAC and CES1A1, CES1A2, and CES2A1 (Fig. 1B). However, the activity in HLM was substantially higher than the sum of those by recombinant AADAC and CES enzymes (Fig. 1B). Other esterases such as paraoxonase and butyrylcholinesterase may participate in the PNPA hydrolysis in HLM.

It has been reported that AADAC is located on the lumen side of endoplasmic reticulum (Frick et al., 2004). This corresponded to the present result that the flutamide hydrolase activity in HLM was substantially higher than in HLC (Fig. 2A). In addition, there was no significant difference between the K_m values of HLM (794 ± 83 μM) and recombinant AADAC wild-type (778 ± 122 μM) (Fig. 2, A and B). This finding also supported the involvement of AADAC in flutamide hydrolysis in human liver. However, the activity was also detected in HLC. It was already known that CES1A and CES2 enzymes are present in HLC (Xu et al., 2002; Tabata et al., 2004), but recombinant CES1A1, CES1A2, and CES2 could not hydrolyze flutamide (Fig. 1C). In addition, it was shown that sialic acid 9-*O*-acetylesterase, an alacepril hydrolase enzyme, purified from rat liver cytosol also could not hydrolyze flutamide (Usui et al., 2003). Therefore, other enzymes that can hydrolyze flutamide may be present in HLC, but the contribution to flutamide hydrolysis would be limited.

To confirm that flutamide hydrolysis in HLM is specifically cata-

Downloaded from dmd.aspetjournals.org at Kanazawa Univ Yakugakubu Lib on September 22, 2009

DMD DRUG METABOLISM AND DISPOSITION aspet

lyzed by AADAC, we performed inhibition analyses by using various chemical inhibitors and heavy metals (Fig. 3). The flutamide hydrolase activity in HLM was inhibited in a BNPP concentration-dependent manner but was not completely inhibited by 1 mM PMSF (residual activity, 56% of control). It is known that the CES1A and CES2 enzyme activities are inhibited in a BNPP concentration-dependent manner and were substantially inhibited by 0.1 mM PMSF (Xie et al., 2002). Therefore, these enzymes would not contribute to the flutamide hydrolysis in HLM. Moreover, the activity was potently inhibited by DFP, eserine, and silver nitrate and moderately inhibited by NaF, disulfiram, and $CuCl_2$. Other inhibitors used in the present study did not cause inhibition. Because DFP and BNPP are organophosphates, general CES inhibitors, it is plausible that DFP also inhibits AADAC. Eserine and NaF are cholinesterase inhibitors (Iwatsubo, 1965; Ciliv and Ozand, 1972; Preuss and Svensson, 1996). It is of interest that flutamide hydrolysis was effectively inhibited by eserine but not by NaF. EDTA and disulfiram are known to be inhibitors of paraoxonase and monoacylglycerol lipase, respectively (Gonzalvo et al., 1997; Labar et al., 2007). Therefore, it was conceivable that these enzymes did not contribute to the flutamide hydrolysis in HLM. The inhibitory specificity of esterases by heavy metals has not been obvious, but in this study we found that AADAC was potently inhibited by $AgNO_3$ and moderately inhibited by $CuCl_2$. Probst et al. (1994) previously reported that the 2-acetylaminofluorene deacetylation catalyzed by AADAC in HLM was inhibited in a BNPP concentration-dependent manner but was not inhibited by increasing the concentrations of PMSF. The inhibition pattern of flutamide hydrolysis by BNPP and PMSF was similar to that of 2-acetylaminofluorene deacetylation.

To investigate the tissue distribution of AADAC mRNA in human normal tissues, real-time RT-PCR was performed (Fig. 4). AADAC mRNA was mainly expressed in human normal liver, small intestine, and colon. In addition, we confirmed that AADAC protein was expressed in human liver and jejunum microsomes but not in human pulmonary and renal microsomes (Fig. 5A). The tissue distribution of AADAC protein corresponded to that of AADAC mRNA. It is of interest that the expression of AADAC protein in jejunum was higher than in liver, although the mRNA expression was opposite. As shown in Fig. 6, there was interindividual variability in AADAC protein level and flutamide hydrolase activity in human liver. The discrepancy may be because of use of liver RNA derived from single donor. In general, the small intestine plays an important role in the first-pass metabolism of therapeutic drugs given orally (Lin et al., 1999). AADAC would play a certain role in the first-pass metabolism of flutamide in small intestine and in liver.

Correlation analysis was performed between the expression level of AADAC protein and the flutamide hydrolase activity using individual HLM samples (Fig. 6). The correlation between the expression level of AADAC and the flutamide hydrolase activity was strongly significant. Although the point appears to show an *x*-axis intercept greater than 0, several individual HLM samples may partially include inactive AADAC protein. The expression level of AADAC protein and the flutamide hydrolase activity were moderately variable. It is feasible that the induction by xenobiotics from the environment or diet and endobiotics, and genetic polymorphism of the *AADAC* gene affect the interindividual variability of the flutamide hydrolase activity and AADAC expression level. However, the regulation mechanisms of human AADAC expression are not fully understood. Saito et al. (2003) previously found 23 SNPs in the *AADAC* gene using DNA samples of 48 Japanese. Among them, only an SNP that was also found in this study (g.13651G > A, c.931G > A) leads to an amino acid change (V281I). However, AADAC variant (V281I) appeared not to alter the enzyme activity (Fig. 3B). It is considered that flutamide hydrolysis is important in the occurrence of hepatotoxicity (Aizawa et al., 2003; Matsuzaki et al., 2006; Ohbuchi et al., 2009). Therefore, the interindividual variability of AADAC might affect the incidence of flutamide-induced hepatotoxicity. Further study on the regulation mechanisms and genetic polymorphisms of human AADAC will be necessary.

In conclusion, we found that human AADAC is a principal enzyme in the flutamide hydrolysis. The present study is the first report of the contribution of human AADAC to the metabolism of a therapeutic drug.

Acknowledgments. We thank Brent Bell for review of the manuscript.

References

Aizawa Y, Ikemoto I, Kishimoto K, Wada T, Yamazaki H, Ohishi Y, Kiyota H, Furuta N, Suzuki H, and Ueda M (2003) Flutamide-induced hepatic dysfunction in relation to steady-state plasma concentrations of flutamide and its metabolites. *Mol Cell Biochem* **252:**149–156.

Block W and Arndt R (1978) Chromatographic study on the specificity of bis-*p*-nitrophenylphosphate in vivo. Identification of labelled proteins of rat liver after intravenous injection of bis-*p*-nitro[14C]phenylphosphate as carboxylesterases and amidases. *Biochim Biophys Acta* **524:**85–93.

Ciliv G and Ozand PT (1972) Human erythrocyte acetylcholinesterase purification, properties and kinetic behavior. *Biochim Biophys Acta* **284:**136–156.

Crawford ED, Eisenberger MA, McLeod DG, Spaulding JT, Benson R, Dorr FA, Blumenstein BA, Davis MA, and Goodman PJ (1989) A controlled trial of leuprolide with and without flutamide in prostatic carcinoma. *N Engl J Med* **321:**419–424.

Fau D, Eugene D, Berson A, Letteron P, Fromenty B, Fisch C, and Pessayre D (1994) Toxicity of the antiandrogen flutamide I isolated rat hepatocytes. *J Pharmacol Exp Ther* **269:**954–962.

Frick C, Atanasov AG, Arnold P, Ozols J, and Odermatt A (2004) Appropriate function of 11β-hydroxysteroid dehydrogenase type 1 in the endoplasmic reticulum lumen is dependent on its N-terminal region sharing similar topological determinants with 50-kDa esterase. *J Biol Chem* **279:**31131–31138.

Goda R, Nagai D, Akiyama Y, Nishikawa K, Ikemoto I, Aizawa Y, Nagata K, and Yamazoe Y (2006) Detection of new *N*-oxidized metabolite of flutamide, *N*-[4-nitro-3-(trifluoromethyl) phenyl]hydroxylamide, in human liver microsomes and urine of prostate cancer patients. *Drug Metab Dispos* **34:**828–835.

Gonzalvo MC, Gil F, Hernández AF, Villanueva E, and Pla A (1997) Inhibition of paraoxonase activity in human liver microsomes by exposure to EDTA, metals and merculials. *Chem Biol Interact* **105:**169–179.

Heymann E and Krisch K (1967) Phospholic acid-bis-(*p*-nitro-phenylester), a new inhibitor of microsomal carboxylesterases. *Hoppe Seylers Z Physiol Chem* **348:**609–619.

Imai T, Taketani M, Shii M, Hosokawa M, and Chiba K (2006) Substrate specificity of carboxylesterase isozymes and their contribution to hydrolase activity in human liver and small intestine. *Drug Metab Dispos* **34:**1734–1741.

Iwatsubo K (1965) Studies on the classification of the enzymes hydrolysing ester-form drugs in liver microsomes. *Jpn J Pharmacol* **15:**244–265.

Johnson G and Moore SW (2000) Cholinesterase-like catalytic antibodies: reaction with substrates and inhibitors. *Mol Immunol* **37:**707–719.

Katchen B and Buxbaum S (1975) Disposition of a new, nonsteroid, antiandrogen, alpha,alpha,alpha-trifluoro-2-methyl-4′-nitro-m-propionotoluidine (Flutamide), in men following a single oral 200 mg dose. *J Clin Endocrinol Metab* **41:**373–379.

Labar G, Bauvois C, Muccioli GG, Wouters J, and Lambert DM (2007) Disulfiram is an inhibitor of human purified monoacylglycerol lipase, the enzyme regulating 2-arachidonoylglycerol signaling. *Chembiochem* **8:**1293–1297.

Laemmli UK (1970) Cleavage of structural proteins during the assembly of the head of bacteriophage T4. *Nature* **227:**680–685.

Lin JH, Chiba M, and Baillie TA (1999) Is the role of the small intestine in first-pass metabolism overemphasized? *Pharmacol Rev* **51:**135–158.

Matsuzaki Y, Nagai D, Ichimura E, Goda R, Tomura A, Doi M, and Nishikawa K (2006) Metabolism and hepatic toxicity of flutamide in cytochrome P450 1A2 knockout SV129 mice. *J Gastroenterol* **41:**231–239.

Mentlein R, Rix-Matzen H, and Heymann E (1988) Subcellular localization of non-specific carboxylesterases, acylcarnitine hydrolase, monoacylglycerol lipase and palmitoyl-CoA hydrolase in rat liver. *Biochim Biophys Acta* **964:**319–328.

Nakajima M, Itoh M, Sakai H, Fukami T, Katoh M, Yamazaki H, Kadlubar FF, Imaoka S, Funae Y, and Yokoi T (2006) CYP2A13 expressed in human bladder metabolically activates 4-aminobiphenyl. *Int J Cancer* **119:**2520–2526.

Ohbuchi M, Miyata M, Nagai D, Shimada M, Yoshinari K, and Yamazoe Y (2009) Role of enzymatic *N*-hydroxylation and reduction in flutamide metabolite-induced liver toxicity. *Drug Metab Dispos* **37:**97–105.

Ozono S, Yamaguchi A, Mochizuki H, Kawakami T, Fujimoto K, Otani T, Yoshida K, Ichinei M, Yamashita T, and Hirao Y (2002) Caffeine test in predicting flutamide-induced hepatic injury in patients with prostate cancer. *Prostate Cancer Prostatic Dis* **5:**128–131.

Preuss CV and Svensson CK (1996) Arylacetamide deacetylase activity towards monoacetyldapsone. *Biochem Pharmacol* **51:**1661–1668.

Probst MR, Beer M, Beer D, Jenö P, Meyer UA, and Gasser R (1994) Human liver arylacetamide deacetylase. Molecular cloning of a novel esterase involved in the metabolic activation of arylamine carcinogens with high sequence similarity to hormone-sensitive lipase. *J Biol Chem* **269:**21650–21656.

Probst MR, Jenö P, and Meyer UA (1991) Purification and characterization of a human liver arylacetamide deacetylase. *Biochem Biophys Res Commun* **177:**453–459.

Downloaded from dmd.aspetjournals.org at Kanazawa Univ Yakugakubu Lib on September 22, 2009

Ross MK and Crow JA (2007) Human carboxylesterases and their role in xenobiotic and endobiotic metabolism. *J Biochem Mol Toxicol* **21**:187–196.
Saito S, Iida A, Sekine A, Kawauchi S, Higuchi S, Ogawa C, and Nakamura Y (2003) Catalog of 680 variations among eight cytochrome P450 (CYP) genes, nine esterase genes, and two other genes in the Japanese population. *J Hum Genet* **48**:249–270.
Sanghani SP, Quinney SK, Fredenburg TB, Davis WI, Murry DJ, and Bosron WF (2004) Hydrolysis of irinotecan and its oxidative metabolites, 7-ethyl-10-[4-N-(5-aminopentanoic acid)-1-piperidino] carbonyloxycamptothecin and 7-ethyl-10-[4-(1-piperidino)-1-amino]-carbonyloxycamptothecin, by human carboxylesterases CES1A1, CES2, and a newly expressed carboxylesterase isoenzyme, CES3. *Drug Metab Dispos* **32**:505–511.
Schulz M, Schmoldt A, Donn F, and Becker H (1988) The pharmacokinetics of flutamide and its metabolites after a single oral dose and during chronic treatment. *Eur J Clin Pharmacol* **34**:633–636.
Tabata T, Katoh M, Tokudome S, Hosakawa M, Chiba K, Nakajima M, and Yokoi T (2004) Bioactivation of capecitabine in human liver: involvement of the cytosolic enzyme on 5′-deoxy-5-fluorocytidine formation. *Drug Metab Dispos* **32**:762–767.
Takai S, Matsuda A, Usami Y, Adachi T, Sugiyama T, Katagiri Y, Tatematsu M, and Hirano K (1997) Hydrolytic profile for ester- or amide-linkage by carboxylesterases pI 5.3 and 4.5 from human liver. *Biol Pharm Bull* **20**:869–873.
Thole Z, Manso G, Salgueiro E, Revuelta P, and Hidalgo A (2004) Hepatotoxicity induced by antiandrogens: a review of the literature. *Urol Int* **73**:289–295.
Tiwari R, Köffel R, and Schneiter R (2007) An acetylation/deacetylation cycle controls the export of sterols and steroids from. *S. cerevisiae. EMBO J* **26**:5109–5119.
Tsuchiya Y, Nakajima M, Kyo S, Kanaya T, Inoue M, and Yokoi T (2004) Human CYP1B1 is regulated by estradiol via estrogen receptor. *Cancer Res* **64**:3119–3125.
Usui S, Kubota M, Iguchi K, Kiho T, Sugiyama T, Katagiri Y, and Hirano K (2003) Sialic acid 9-*O*-acetylesterase catalyzes the hydrolyzing reaction from alacepril to deacetylalacepril. *Pharm Res* **20**:1309–1316.
Xie M, Yang D, Liu L, Xue B, and Yan B (2002) Human and rodent carboxylesterase: immunorelatedness, overlapping substrate specificity, differential sensitivity to serine enzyme inhibitors, and tumor-related expression. *Drug Metab Dispos* **30**:541–547.
Xu G, Zhang W, Ma MK, and McLeod HL (2002) Human carboxylesterase 2 is commonly expressed in tumor tissue and is correlated with activation of irionotecan. *Clin Cancer Res* **8**:2605–2611.
Yamaori S, Fujiyama N, Kushihara M, Funahashi T, Kimura T, Yamamoto I, Sone T, Isobe M, Ohshima T, Matsumura K, et al. (2006) Involvement of human blood arylesterases and liver microsomal carboxylesterases in nafamostat hydrolysis. *Drug Metab Pharmacokinet* **21**:147–155.

Address correspondence to: Tsuyoshi Yokoi, Drug Metabolism and Toxicology, Faculty of Pharmaceutical Sciences, Kanazawa University, Kakuma-machi, Kanazawa 920-1192, Japan. E-mail: tyokoi@kenroku.kanazawa-u.ac.jp

DMD DRUG METABOLISM AND DISPOSITION aspet

Downloaded from dmd.aspetjournals.org at Kanazawa Univ Yakugakubu Lib on September 22, 2009

Biochemical Pharmacology 79 (2010) 1045–1052

Contents lists available at ScienceDirect

Biochemical Pharmacology

journal homepage: www.elsevier.com/locate/biochempharm

Human CYP2E1 is regulated by miR-378

Takuya Mohri [a], Miki Nakajima [a], Tatsuki Fukami [a], Masataka Takamiya [b], Yasuhiro Aoki [b], Tsuyoshi Yokoi [a,*]

[a] Drug Metabolism and Toxicology, Faculty of Pharmaceutical Sciences, Kanazawa University, Kakuma-machi, Kanazawa 920-1192, Japan
[b] Department of Legal Medicine, Iwate Medical University School of Medicine, 19-1 Uchimaru, Morioka 020-8505, Japan

ARTICLE INFO

Article history:
Received 26 September 2009
Accepted 20 November 2009

Keywords:
miRNA
Cytochrome P450
Post-transcriptional regulation
Liver
Interindividual variability

ABSTRACT

Human CYP2E1 is one of the pharmacologically and toxicologically important cytochrome P450 isoforms. Earlier studies have reported that the CYP2E1 expression is extensively regulated by post-transcriptional and post-translational mechanisms, but the molecular basis remains unclear. In the present study, we examined the possibility that microRNA may be involved in the post-transcriptional regulation of human CYP2E1. In silico analysis identified a potential recognition element of miR-378 (MRE378) in the 3′-untranslated region (UTR) of human CYP2E1 mRNA. Luciferase assays using HEK293 cells revealed that the reporter activity of the plasmid containing the MRE378 was decreased by co-transfection of precursor miR-378, indicating that miR-378 functionally recognized the MRE378. We established two HEK293 cell lines stably expressing human CYP2E1 including or excluding 3′-UTR. When the precursor miR-378 was transfected into the cells expressing human CYP2E1 including 3′-UTR, the CYP2E1 protein level and chlorzoxazone 6-hydroxylase activity were significantly decreased, but were not in the cells expressing CYP2E1 excluding 3′-UTR. In both cell lines, the CYP2E1 mRNA levels were decreased by overexpression of miR-378, but miR-378 did not affect the stability of CYP2E1 mRNA. In a panel of 25 human livers, no positive correlation was observed between the CYP2E1 protein and CYP2E1 mRNA levels, supporting the post-transcriptional regulation. Interestingly, the miR-378 levels were inversely correlated with the CYP2E1 protein levels and the translational efficiency of CYP2E1. In conclusion, we found that human CYP2E1 expression is regulated by miR-378, mainly via translational repression. This study could provide new insight into the unsolved mechanism of the post-transcriptional regulation of CYP2E1.

© 2009 Elsevier Inc. All rights reserved.

1. Introduction

Human cytochrome P450 (CYP) 2E1 catalyzes the metabolism of numerous low molecular-weight xenobiotics including drugs (e.g., acetaminophen, isoniazid), organic solvents (e.g., ethanol, acetone, carbon tetrachloride), and procarcinogens (e.g., *N*-nitrosodimethylamine) [1]. CYP2E1 is induced by its own substrates such as isoniazid, ethanol, and acetone, resulting in the enhancement of their metabolism [2]. It should be noted that the induction of CYP2E1 protein by these chemicals was not necessarily accompanied by an increase of CYP2E1 mRNA level [3]. The proposed mechanisms for the induction of CYP2E1 are the stabilization of mRNA [4] or protein [5]. Previously, Sumida et al. [6] reported that the CYP2E1 mRNA levels in 15 human liver samples were not positively correlated with the chlorzoxazone 6-hydroxylase activities, which is a probe activity of CYP2E1. In addition, special attention should be paid to the fact that CYP2E1 is the most abundant isoform among all P450s in human liver (56% of total P450) at the mRNA level, followed by CYP2C9, CYP2C8 and CYP3A4 (8–11% of total P450) [7], whereas it is the fourth most abundant isoform (about 7% of total P450) at the protein level after CYP3A (30% of total P450), CYP2C (20% of total P450), and CYP1A2 (about 13% of total P450) [8]. Collectively, the post-transcriptional regulation would be responsible for not only the inducible but also the constitutive expression of CYP2E1 in liver. However, the molecular basis of the human CYP2E1 regulation largely remains unknown, in contrast to the other human P450s for which much progress has been made in understanding the regulation mechanisms at the transcriptional level.

To uncover the molecular mechanism of the post-transcriptional regulation of CYP2E1, we sought to determine whether microRNA (miRNA) might be involved in the regulation of CYP2E1. MiRNAs, an evolutionarily conserved class of endogenous ~22-nucleotide non-coding RNAs, recognize the 3′-untranslated region (3′-UTR) of the target mRNA and cause translational repression or mRNA degradation [9]. The regulation by miRNAs is involved in

* Corresponding author. Tel.: +81 76 234 4407; fax: +81 76 234 4407.
E-mail address: nmiki@kenroku.kanazawa-u.ac.jp (T. Yokoi).

0006-2952/$ – see front matter © 2009 Elsevier Inc. All rights reserved.
doi:10.1016/j.bcp.2009.11.015

diverse biological processes, including development, cell proliferation, differentiation, apoptosis, and cancer initiation and progression [10–12]. The human genome may contain up to 1000 miRNAs and 30% of human mRNAs are predicted to be targets of miRNAs [13]. However, the targets of miRNAs largely remain to be identified. Based on the evidence of the post-transcriptional regulation, we investigated whether miRNAs might be involved in the regulation of human CYP2E1.

2. Materials and methods

2.1. Chemicals and reagents

Chlorzoxazone, 6-hydroxychlorzoxazone, and coumarin were from Sigma–Aldrich (St. Louis, MO). $NADP^+$, glucose-6-phosphate, and glucose-6-phosphate dehydrogenase were purchased from Oriental Yeast (Tokyo, Japan). The pGL3-promoter vector, phRL-TK plasmid, pTARGET vector, and a dual-luciferase reporter assay system were purchased from Promega (Madison, WI). LipofectAMINE2000 and LipofectAMINE RNAiMAX were from Invitrogen (Carlsbad, CA). Pre-miR miRNA Precursors for miR-378 and negative control #1 were from Ambion (Austin, TX). RNAiso, random hexamer, and SYBR Premix Ex Taq were from Takara (Shiga, Japan). ROX was purchased from Stratagene (La Jolla, CA). ReverTra Ace was obtained from Toyobo (Osaka, Japan). All primers and oligonucleotides were commercially synthesized at Hokkaido System Sciences (Sapporo, Japan). G418 was obtained from Wako Pure Chemicals (Osaka, Japan). α-Amanitin was purchased from Calbiochem (San Diego, CA). Goat anti-human CYP2E1 polyclonal antibodies and rabbit anti-human GAPDH polyclonal antibodies were from Daiichi Pure Chemicals (Tokyo, Japan) and IMGENEX (San Diego, CA), respectively. Restriction enzymes were from Takara, Toyobo, and New England Biolabs (Ipswich, MA). All other chemicals and solvents were of the highest grade commercially available.

2.2. Construction of reporter plasmids

Various fragments were inserted into the *Xba* I site, downstream of the luciferase gene in the pGL3-promoter vector. The sequence from +1559 to +1580 of the human CYP2E1 mRNA (5′-TCA AAT TGT TTG AGG TCA GGA T-3′) was termed the miR-378 recognition element (MRE378). A fragment containing three copies of the MRE378, 5′-CTA GAG TTT *TCA AAT TGT TTG AGG TCA GGA* TTT CTC GTT *TTC AAA TTG TTT GAG GTC AGG ATT* TCT CGT TTT *CAA ATT GTT TGA GGT CAG GAT* TTC TCT-3′ (MRE378 is italicized), was cloned into the pGL3-promoter vector (pGL3/3xMRE). The complementary sequence of three copies of the MRE378 was also cloned into the pGL3-promoter plasmid (pGL3/3xMRE-Rev). A fragment containing the perfectly matching sequence with the mature miR-378, 5′-CTA *GAA CAC AGG ACC TGG AGT CAG GAG* T-3′ (the matching sequence of miR-378 is italicized), was cloned into the pGL3-promoter vector (pGL3/c-378). A fragment from +1549 to +1627 of the human CYP2E1 mRNA containing the MRE378 was cloned into the pGL3-promoter vector, resulting in single (pGL3/UTR1) and double (pGL3/2xUTR1) insertion. A fragment +1627 to +1657 excluding the MRE378 was also cloned into the pGL3-promoter vector, resulting in single (pGL3/UTR2) insertion. DNA sequencing analyses using Long-Read Tower DNA sequencer (GE Healthcare Bio-Sciences, Piscataway, NJ) confirmed the nucleotide sequences of these constructed plasmids.

2.3. Cell culture and luciferase assay

Human embryonic kidney cell line HEK293 was obtained from the American Type Culture Collection (Manassas, VA). HEK293 cells were cultured in Dulbecco's modified Eagle's medium (DMEM) (Nissui Pharmaceutical, Tokyo, Japan) supplemented with 4.5 g/l glucose, 10 mM HEPES, and 10% fetal bovine serum (Invitrogen). These cells were maintained at 37 °C under an atmosphere of 5% CO_2–95% air.

Various luciferase reporter plasmids (pGL3) were transiently transfected with phRL-TK plasmid into the HEK293 cells. Briefly, the day before transfection, the cells were seeded into 24-well plates. After 24 h, 170 ng of pGL3 plasmid, 30 ng of phRL-TK plasmid and the precursors for miR-378 or control were co-transfected using LipofectAMINE 2000. After incubation for 48 h, the cells were lysed with a passive lysis buffer and then the luciferase activity was measured with a luminometer (Wallac, Turku, Finland) using the dual-luciferase reporter assay system.

2.4. Establishment of two HEK293 cell lines stably expressing human CYP2E1 including or excluding 3′-UTR

A fragment containing the full-length coding region as well as 3′-UTR of the human CYP2E1 cDNA (from +34 to +1667) was amplified by PCR using the primers of 5′-ATG TCT GCC CTC GGA GTC AC-3′ and 5′-AAA ATA ATC ATG TGA TGA TTT ATT TAT ATT CTG GG-3′. A fragment containing only the full-length coding region of the human CYP2E1 cDNA (from +34 to +1516) was also amplified using the primers of 5′-ATG TCT GCC CTC GGA GTC AC-3′ and 5′-CTC ATG AGC GGG GAA TGA CA-3′. These fragments were subcloned into the pTARGET vector and the resultants were termed pTARGET/CYP2E1 + UTR and pTARGET/CYP2E1. The nucleotide sequences of the plasmids were confirmed by DNA sequencing analyses. HEK293 cells were seeded into 24-well plates, and 500 ng of pTARGET/CYP2E1 + UTR or pTARGET/CYP2E1 plasmids were transfected using LipofectAMINE 2000 according to the manufacturer's protocols. At 48 h post-transfection, the cells were passaged and subsequently grown in medium containing 400 μg/ml G418, and diluted from 1:10 to 1:1000. The selective medium was changed every 3–4 days and individual G418-tolerable colonies were selected after 2 weeks in culture. Tolerable clones were screened by immunoblotting and measurement of enzyme activity. We confirmed that the CYP2E1 protein level and the enzyme activity were sustained regardless of the repeated subculture.

2.5. Transfection of precursor for miR-378 into HEK293/2E1 + UTR cells and HEK293/2E1 cells and preparation of cell homogenates and total RNA

The precursor for miR-378 was transfected into the HEK293/2E1 + UTR cells and HEK293/2E1 cells as follows: the day before transfection, the cells were seeded into 6- or 12-well plates. After 24 h, 10 nM precursors for miR-378 or control were transfected into HEK293/2E1 + UTR and HEK293/2E1 cells using LipofectAMINE RNAiMAX. After incubation for 48 h, the cells were harvested and suspended in a small amount of TGE buffer [10 mM Tris–HCl, 20% glycerol, 1 mM EDTA (pH 7.4)] and disrupted by freeze–thawing three times. Total RNA was prepared using RNAiso according to the manufacturer's protocols.

2.6. Determination of the half-life of CYP2E1 mRNA

The HEK293/2E1 + UTR cells and HEK293/2E1 cells transfected with the precursor for miR-378 or control as described above were simultaneously treated with 2 μg/ml α-amanitin. Total RNA was prepared at 1, 2, 3, 4, 5, 6 and 9 h later. The CYP2E1 mRNA levels were determined by real-time RT-PCR as described below.

2.7. Human livers and preparation of microsomes and total RNA

Human liver samples from 15 donors were obtained from Human and Animal Bridging (HAB) Research Organization (Chiba, Japan) which is in partnership with the National Disease Research Interchange (NDRI, Philadelphia, PA), and those from 10 donors were obtained from autopsy materials that were discarded after pathological investigation [14]. The use of the human livers was approved by the Ethics Committees of Kanazawa University (Kanazawa, Japan) and Iwate Medical University (Morioka, Japan). Microsomes fractions were prepared from 25 human livers according to the method described previously [15]. The protein concentration was determined using Bradford protein assay reagent (Bio-Rad, Hercules, CA) with γ-globulin as a standard. Total RNA was prepared using RNAiso and the integrity of the RNA was assessed by estimating the ratio of the band density of 28S and 18S rRNA.

2.8. SDS-PAGE and Western blot analyses of CYP2E1

Cell homogenates from HEK293/2E1 + UTR cells or HEK293/2E1 cells (10–40 μg) and human liver microsomes (3 μg) were separated on 10% SDS-PAGE and transferred to Immobilon-P transfer membrane (Millipore, Billerica, MA). The membrane was probed with goat anti-human CYP2E1 antibody. Biotinylated anti-goat IgG and a Vectastain ABC kit (Vector Laboratories, Burlingame, CA) were used for diaminobenzidine staining. As for cell homogenates from the HEK293 expression systems, the CYP2E1 protein level was normalized with the GAPDH protein level. As for human liver microsomes, a standard curve using recombinant human CYP2E1 expressed in baculovirus-infected insect cells (BD Gentest, Worburn, MA) was used to determine the absolute expression level of CYP2E1 protein. The quantitative analysis was performed using ImageQuant TL Image Analysis software (GE Healthcare Bio-Sciences).

2.9. Enzyme activity

Chlorzoxazone 6-hydroxylase activity was determined as follows: a typical incubation mixture (final volume of 0.2 ml) contained 50 mM potassium phosphate buffer (pH 7.4), 500 μM chlorzoxazone, and 0.5 mg/ml cell homogenates from HEK293/2E1 + UTR cells or HEK293/2E1 cells or human liver microsomes. The reaction was initiated by the addition of the NADPH-generating system (0.5 mM $NADP^+$, 5 mM glucose-6-phosphate, 5 mM $MgCl_2$, and 1 U/ml glucose-6-phosphate dehydrogenase) after 2 min preincubation at 37 °C. After the 10–30 min incubation at 37 °C, the reaction was terminated by the addition of 10 μl of ice-cold 10% perchloric acid. Coumarin (0.25–1 nmol) was added as an internal standard. After removal of the protein by centrifugation at 10,000 rpm for 5 min, a portion of the supernatant was subjected to high-performance liquid chromatography

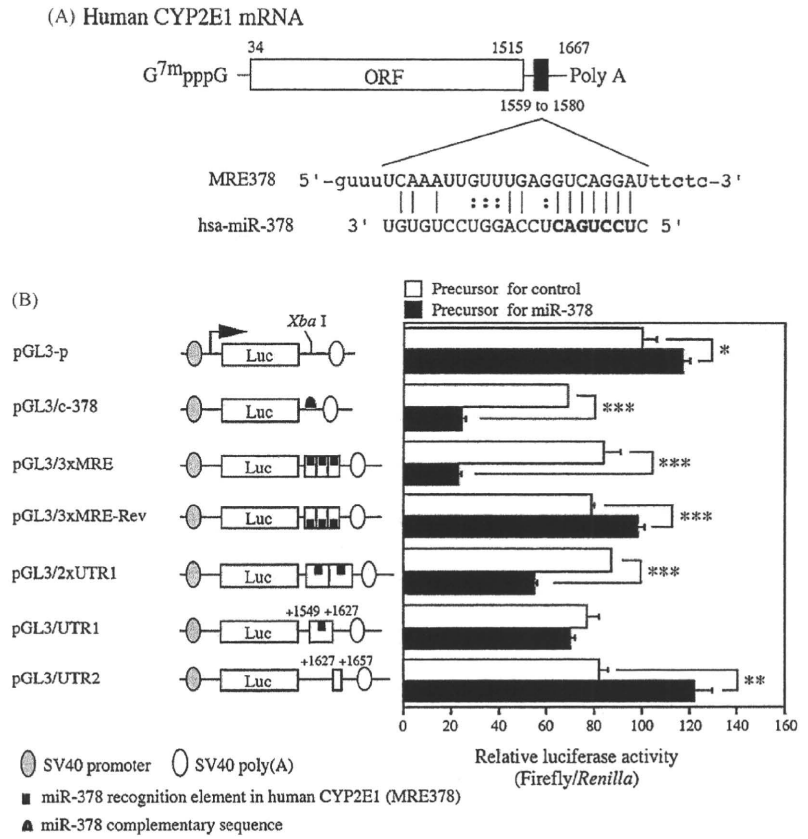

Fig. 1. Luciferase assay using the plasmids containing the MRE378 in the 3′-UTR of human CYP2E1 mRNA. Schematic representation of human CYP2E1 mRNA and the predicted target sequence of miR-378 (A). The numbering refers to the 5′ end of mRNA as 1, and the coding region is from +34 to +1515. MRE378 (from +1559 to +1580) is located on the 3′-UTR of human CYP2E1 mRNA. *bold letters*, seed sequence. Luciferase assays using the reporter plasmids containing various fragments downstream of the firefly luciferase gene (B). The reporter plasmids (170 ng) were transiently transfected with phRL-TK plasmid (30 ng) and 20 nM precursors for miR-378 or negative control #1 (control) into HEK293 cells. The firefly luciferase activity for each construct was normalized with the *Renilla* luciferase activities. Values are expressed as percentages of the relative luciferase activity of pGL3-p plasmid. Each column represents the mean ± SD of three independent experiments. $^*P < 0.05$, $^{**}P < 0.01$, $^{***}P < 0.001$, compared with the precursor for control.

(HPLC). The HPLC analyses were performed using an L-7100 pump (Hitachi, Tokyo, Japan), an L-7200 autosampler (Hitachi), an L-7405 UV detector (Hitachi), and a D-2500 chromato-integrator (Hitachi) equipped with a Mightysil RP-18 C18 GP (4.6 mm × 150 mm, 5 μm) column (Kanto Chemical, Tokyo, Japan). The eluent was monitored at 295 nm with a noise-base clean Uni-3 (Union, Gunma, Japan). The mobile phase was 28% methanol containing 50 mM potassium phosphate (pH 4.2). The flow rate was 1.0 ml/min. The column temperature was 35 °C. The quantification of the metabolites was performed by comparing the HPLC peak height with that of authentic standards with reference to an internal standard.

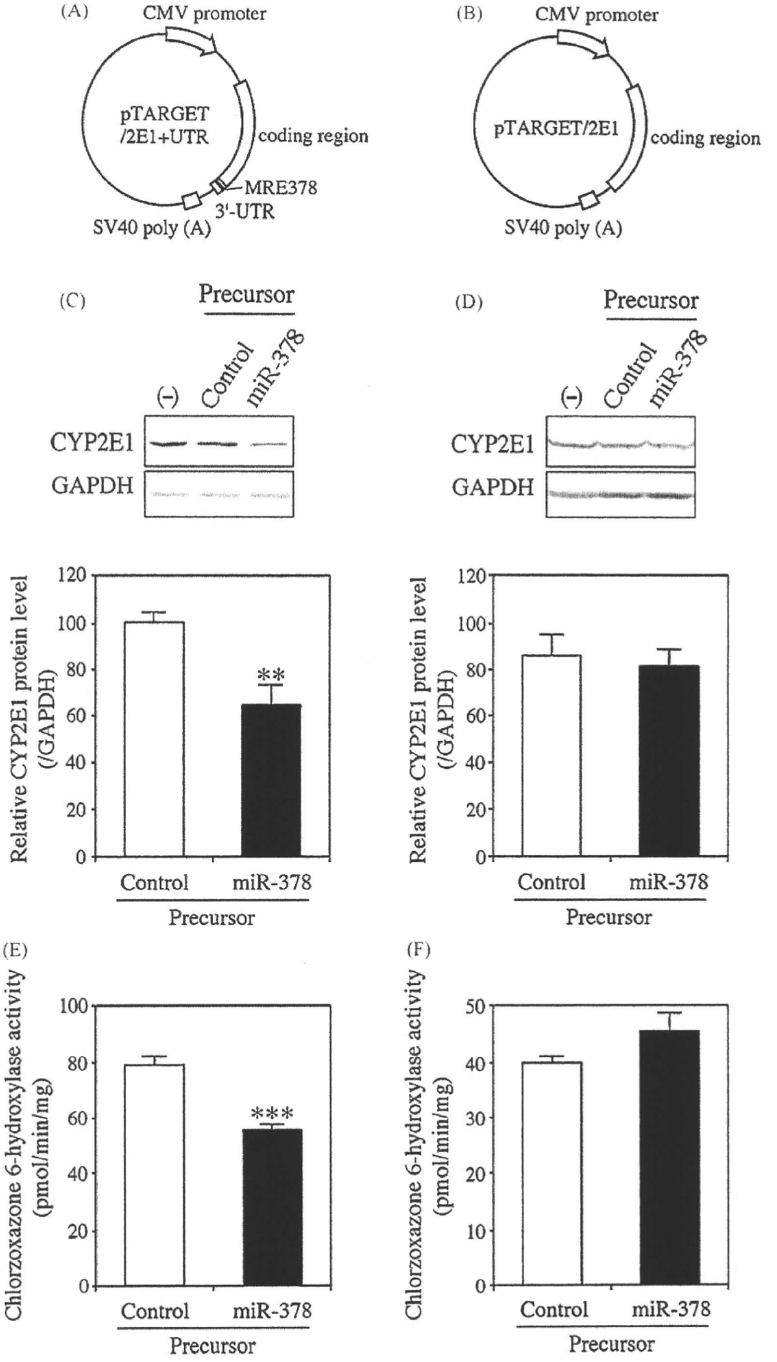

Fig. 2. Effects of overexpression of miR-378 on protein level and enzyme activity of CYP2E1. Schematic representation of the CYP2E1 expression plasmids including (A) or excluding (B) 3′-UTR of CYP2E1 (pTARGET/2E1-UTR or pTARGET/2E1). The CYP2E1 protein levels in HEK293/2E1 + UTR (C) and HEK293/2E1 (D) cells 48 h after the transfection of 10 nM precursors for miR-378 or negative control #1 (control). The CYP2E1 protein levels were determined by Western blot analysis and were normalized with the GAPDH protein level. Values are expressed as percentages relative to no transfection (−). Each column represents the mean ± SD of three independent experiments. $^{**}P < 0.01$, compared with the precursor for control. Enzyme activity of CYP2E1 in HEK293/2E1 + UTR (E) and HEK293/2E1 (F) cells 48 h after the transfection of 10 nM precursors for miR-378 or control. Chlorzoxazone 6-hydroxylase activity was measured using the cell homogenate at a substrate concentration of 500 μM. The control activities in homogenates from non-treated HEK293/2E1 + UTR (E) and HEK293/2E1 (F) cells were 70.5 ± 8.5 and 41.9 ± 1.0 pmol/min/mg, respectively. Each column represents the mean ± SD of three independent experiments. $^{***}P < 0.001$, compared with the precursor for control.

2.10. Real-time RT-PCR for CYP2E1

The cDNA was synthesized from total RNA using ReverTra Ace. The CYP2E1 mRNA levels were quantified by real-time RT-PCR using the Mx3000P™ (Stratagene). The forward and reverse primers for CYP2E1 mRNA were 5′-ACG GTA TCA CCG TGA CTG TGG-3′ and 5′-GCA TCT CTT GCC TAT CCT TGA-3′, respectively. A 1 μl portion of the reverse-transcribed mixture was added to a PCR mixture containing 10 pmol of each primer, 12.5 μl of SYBR Premix Ex Taq solution and 75 nM ROX in a final volume of 25 μl. The PCR condition was as follows: after an initial denaturation at 95 °C for 30 s, the amplification was performed by denaturation at 94 °C for 4 s, annealing and extension at 58 °C for 20 s for 45 cycles. The PCR product was digested with appropriate restriction enzymes to confirm that the amplicon was indeed CYP2E1. The CYP2E1 mRNA levels were normalized with GAPDH mRNA as described previously [16].

2.11. Real-time RT-PCR for mature miR-378

The expression levels of mature miR-378 in human livers were determined by TaqMan quantitative real-time PCR using the TaqMan microRNA assay (Applied Biosystems, Foster City, CA). The cDNA templates were prepared with the TaqMan microRNA Reverse Transcription kit which utilized the stem-loop reverse primers according to the manufacturer's protocols. After the reverse transcription reaction, the product was mixed with TaqMan Universal PCR Master Mix and TaqMan MicroRNA assay containing the forward and reverse primers as well as the TaqMan probe for miR-378. The PCR condition was as follows: after an initial denaturation at 95 °C for 10 min, the amplification was performed by denaturation at 95 °C for 15 s, annealing and extension at 60 °C for 60 s for 40 cycles. The expression levels of U6 small nuclear RNA (U6 snRNA) were also determined by TaqMan quantitative real-time PCR and were used to normalize the miR-378 levels.

2.12. Statistical analyses

Statistical significance was determined by unpaired, two-tailed student's *t*-test. Correlation analyses were performed by Pearson's product-moment method. A value of $P < 0.05$ was considered statistically significant.

3. Results

3.1. A miR-378 complementary sequence on the 3′-UTR of human CYP2E1 mRNA

The length of the 3′-UTR of human CYP2E1 is 152 bp. Computational prediction using miRBase Target database (http://microrna.sanger.ac.uk/) [17] indicated that 24 miRNAs including miR-378, miR-607, miR-223, and miR-105 share complementarity with sequences in the 3′-UTR. Meanwhile, when a Targetscan (http://www.targetscan.org/) was used, 6 miRNAs were found to share complementarity. The common miRNAs predicted in both web sites were only miR-378 and miR-607. We focused on miR-378 because it showed higher complementarity with the CYP2E1 mRNA (score 18.31 and energy −16.95) than the others. Fig. 1A shows the alignment of hsa-miR-378 with 3′-UTR of human CYP2E1 mRNA drawn using RNAhybrid (http://bibiserv.techfak.uni-bielefeld.de/rnahybrid/) [18]. We termed the sequence from +1559 to +1580 of the human CYP2E1 mRNA miR-378 recognition element (MRE378). We investigated whether the miR-378 might be involved in the regulation of CYP2E1 via the MRE378.

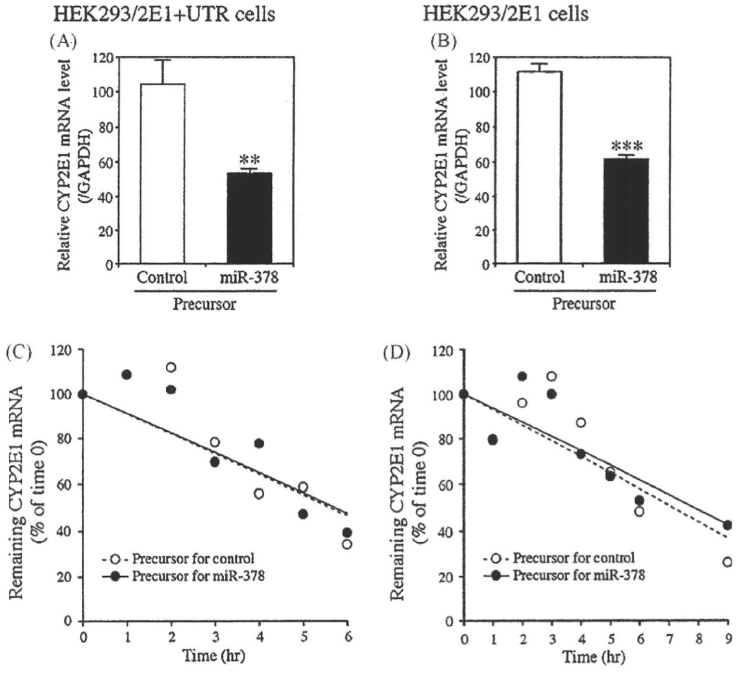

Fig. 3. Effects of overexpression of miR-378 on the CYP2E1 mRNA level and its stability. The CYP2E1 mRNA levels in HEK293/2E1 + UTR (A) and HEK293/2E1 (B) cells 48 h after the transfection of 10 nM precursors for miR-378 or negative control #1 (control). The CYP2E1 mRNA levels were determined by real-time RT-PCR and normalized with GAPDH mRNA. Values are expressed as percentages relative to no transfection. Each column represents the mean ± SD of three independent experiments. $^{**}P < 0.01$, $^{***}P < 0.001$, compared with the precursor for control. Stability of the CYP2E1 mRNA in the HEK293/2E1 + UTR (C) and HEK293/2E1 (D) cells. The cells transfected with 10 nM precursors for miR-378 or negative control #1 (control) were simultaneously treated with 2 μg/ml α-amanitin. Total RNA was prepared at 1, 2, 3, 4, 5, 6 and 9 h later. The CYP2E1 mRNA levels were determined by real-time RT-PCR and normalized with GAPDH mRNA. The amounts of mRNA at time 0 (the time of addition of α-amanitin) in each group (miR-378 or control treated) were assigned a value of 100%, and all other values at different time points were expressed as percentages of the time 0 value. Data are the mean of two independent experiments.

3.2. Luciferase assay to investigate whether the MRE378 is functional

To investigate whether MRE378 is functional in the regulation by miR-378, luciferase assays were performed using HEK293 cells (Fig. 1B) that barely express miR-378 (data not shown). We first confirmed that the luciferase activity of the pGL3/c-378 plasmid, which contains the miR-378 complementary sequence, was significantly ($P < 0.001$) decreased (35% of control) by the co-transfection of the precursor for miR-378. The luciferase activity of the pGL3/3xMRE plasmid containing three copies of the MRE378 was significantly ($P < 0.001$) decreased (27% of control) by the overexpression of miR-378, whereas that of the pGL3/3xMRE-Rev plasmid with the inverted MRE378 was not. The luciferase activity of pGL3/UTR1 plasmid containing the single insertion of MRE378 was decreased by the overexpression of miR-378 (91% of control), although the difference was statistically insignificant. The luciferase activity of the pGL3/2xUTR1 plasmid containing the double insertion of the MRE378 was significantly ($P < 0.001$) decreased (63% of control) by the overexpression of miR-378. In contrast, the luciferase activity of the pGL3/UTR2 plasmid containing the 3′-UTR sequence excluding MRE378 was increased by the overexpression of miR-378, although the reason is not clear. The luciferase activity of the pGL3-p plasmid was also increased by the overexpression of miR-378. Possibly, miR-378 might affect some factors for the SV40 promoter. This may suggest that the repressive effects of miR-378 on 3′-UTR of the reporter gene were underestimated. The results presented here suggest that miR-378 functionally recognized the MRE378 on the human CYP2E1 mRNA.

3.3. Effects of overexpression of miR-378 on protein level and enzyme activity of CYP2E1

Since the CYP2E1 expression levels in cell lines derived from human cancers are too low to be detected by Western blot analysis, we sought to establish cell lines expressing CYP2E1. To examine the role of MRE378 on the 3′-UTR of CYP2E1 gene, two HEK293 transfectants with pTARGET/CYP2E1 + UTR (Fig. 2A) and pTARGET/CYP2E1 (Fig. 2B) plasmids were established. When the miR-378 was overexpressed in HEK293/2E1 + UTR cells, the CYP2E1 protein level was significantly ($P < 0.01$) decreased (60% of control) (Fig. 2C). The chlorzoxazone 6-hydroxylase activity was also significantly ($P < 0.01$) decreased (70% of control) by the overexpression of miR-378 (Fig. 2E). In contrast, the overexpression of miR-378 did not affect the CYP2E1 protein level (Fig. 2D) and enzyme activity (Fig. 2F) in the HEK293/2E1 cells. These results clearly indicated that 3′-UTR including MRE378 plays an important role in the miR-378-dependent down-regulation of CYP2E1. In silico searches raised other candidates including miR-223 (score 17.51, energy −16.47) and miR-105 (score 16.97, energy −15.39) for human CYP2E1. However, the co-transfection of precursor for miR-223 or miR-105 into the HEK293/2E1 + UTR cells did not cause a decrease of the CYP2E1 protein (data not shown). Thus, we found that human CYP2E1 is specifically regulated by miR-378.

3.4. Effects of overexpression of miR-378 on the CYP2E1 mRNA level and its degradation

To investigate if the down-regulation of CYP2E1 by miR-378 involves mRNA degradation, we determined the CYP2E1 mRNA

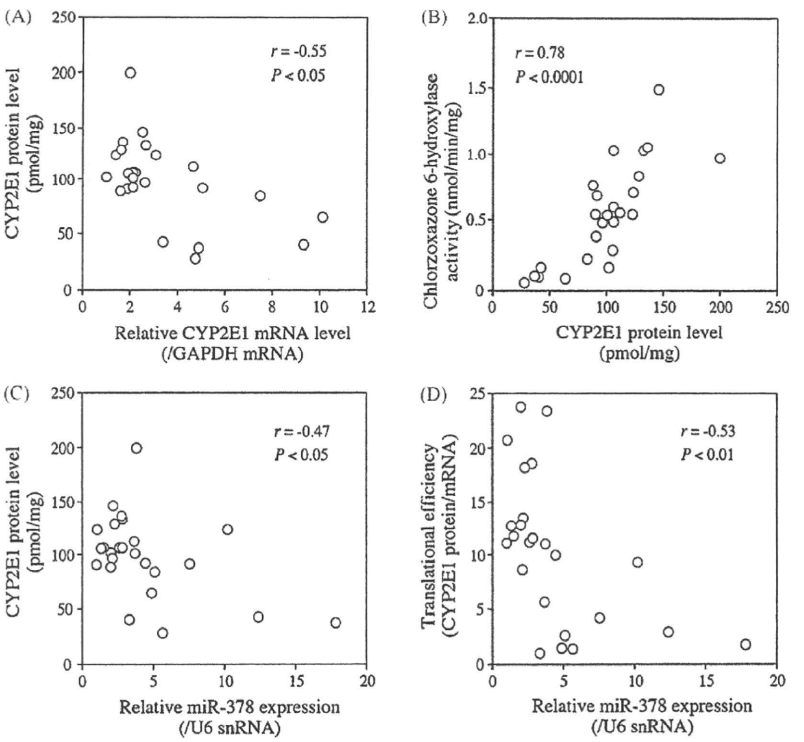

Fig. 4. Relationship between the miR-378, CYP2E1 mRNA, and CYP2E1 protein levels and enzyme activity in human livers. Relationship between the CYP2E1 mRNA and protein levels (A), the CYP2E1 protein levels and chlorzoxazone 6-hydroxylase activities (B), the miR-378 and CYP2E1 protein levels (C), and the miR-378 levels and translational efficiency of CYP2E1 (CYP2E1 protein/mRNA ratio) (D). The expression levels of miR-378 and CYP2E1 mRNA in a panel of 25 human livers were determined by real-time RT-PCR and normalized with U6 snRNA levels and GAPDH mRNA levels, respectively. The values represent the levels relative to that of the lowest sample. The absolute CYP2E1 protein levels were determined by Western blot analysis using a standard curve with recombinant human CYP2E1 protein. The chlorzoxazone 6-hydroxylase activity was measured using human liver microsomes at a substrate concentration of 500 μM. Data are the mean of two independent experiments.

levels. When the miR-378 was overexpressed in HEK293/2E1 + UTR cells, the CYP2E1 mRNA level was significantly ($P < 0.01$) decreased (51% of control) (Fig. 3A). Similarly, the CYP2E1 mRNA level was also significantly ($P < 0.001$) decreased (55% of control) in HEK293/2E1 cells (Fig. 3B). Next, we investigated whether miR-378 affects the stability of the CYP2E1 mRNA. When the HEK293/2E1 + UTR cells were treated with α-amanitin, an inhibitor of transcription, the half-life of the CYP2E1 mRNA was estimated to be 5.6 h (Fig. 3C). The overexpression of miR-378 did not affect the half-life. The half-life of the CYP2E1 mRNA in the HEK293/2E1 cells was 7.1 h (Fig. 3D), and it was not affected by the overexpression of miR-378. These results suggest that miR-378 did not affect the degradation of CYP2E1 mRNA.

3.5. Relationship between the expression levels of miR-378, CYP2E1 mRNA, and CYP2E1 protein in human livers

To investigate the impact of the miR-378 on the CYP2E1 regulation in human livers, we examined the relationship between the expression levels of miR-378, CYP2E1 mRNA and protein as well as enzyme activity using a panel of 25 human livers. The CYP2E1 mRNA levels showed 10-fold interindividual variability. The CYP2E1 protein levels (27.7–199.7 pmol/mg, 7-fold variability) were significantly ($r = 0.78$, $P < 0.0001$) correlated with the chlorzoxazone 6-hydroxylase activities (0.05–1.49 nmol/min/mg, 30-fold variability) (Fig. 4B), but were inversely correlated with the CYP2E1 mRNA levels ($r = -0.55$, $P < 0.05$) (Fig. 4A), supporting the involvement of post-transcriptional regulation. Interestingly, the miR-378 levels (18-fold variability) showed a significant inverse correlation with the CYP2E1 protein levels ($r = -0.47$, $P < 0.05$) (Fig. 4C) and the translational efficiency of CYP2E1 (CYP2E1 protein/mRNA ratio) ($r = -0.53$, $P < 0.01$) (Fig. 4D). These results suggest that miR-378-dependent regulation has a great impact on the CYP2E1 expression in human livers.

4. Discussion

Earlier studies have reported that the induction of CYP2E1 seems to be regulated at the post-transcriptional or post-translational levels by the stabilization of mRNA [4] or protection against the rapid degradation of protein [5,19]. To obtain a clue towards understanding the mechanisms, we investigated the possibility that miRNAs may be involved in the regulation of human CYP2E1. As the results, we found that the miR-378 is involved in the post-transcriptional regulation of CYP2E1.

The overexpression of miR-378 significantly decreased the CYP2E1 protein level and enzyme activity in the cells expressing CYP2E1 including 3′-UTR, but not in the cells expressing CYP2E1 excluding 3′-UTR indicating that the 3′-UTR plays a role in the miR-378-dependent repression. Unexpectedly, the CYP2E1 mRNA levels in both cell lines were decreased by the overexpression of miR-378. However, the miR-378 did not facilitate the degradation of the CYP2E1 mRNA. Therefore, the down-regulation of CYP2E1 by miR-378 would mainly be due to the translational repression, not the mRNA degradation. The decrease of the CYP2E1 mRNA levels in the absence of α-amanitin (Fig. 3A and B) suggests the possibility that miR-378 affects the transcription of CYP2E1. To examine the possibility that the miR-378 might affect the CMV promoter activity, we utilized other heterologous expression systems with the pTARGET vector (i.e., HEK/CYP2A6, HEK/UGT1A3, and HEK/UGT1A4). These heterologously expressed mRNA levels were not affected by the overexpression of miR-378 (data not shown). Therefore, it was concluded that the decrease of CYP2E1 mRNA level by miR-378 was not due to the effects on the CMV promoter. Although the cause of the decrease of CYP2E1 mRNA by miR-378 remains to be clarified, a major mechanism of the down-regulation of CYP2E1 by miR-378 would be the translational repression, supported by the inverse correlation between the miR-378 levels and translational efficiency of CYP2E1 (Fig. 4C).

The sequences of mature miR-378 are completely conserved among human, rat, and mouse, but the sequence of the 3′-UTR of CYP2E1 is poorly conserved. Therefore, the regulation of CYP2E1 by miR-378 would be specific in human. Further study is needed to determine whether other miRNAs except miR-378 might be involved in the regulation of the CYP2E1 in other species.

As for miR-378, it has been reported that it promotes cell survival, tumor growth, and angiogenesis by repressing the expression of Sufu (suppressor of fused) and Fus-1, which are tumor suppressors [20]. Hua et al. [21] have reported that miR-378 binds to the 3′-UTR of vascular endothelial growth factor (VEGF) competing with other miRNAs and promotes the expression of VEGF. In addition to these studies, we provide new information concerning the role of miR-378 from pharmacological and toxicological aspects.

The gene coding miR-378 is within the intron 1 of the *peroxisome-proliferator-activated receptor-γ co-activator 1β (PGC1β)* gene on human chromosome 5q33.1 (http://microrna.sanger.ac.uk/sequences/). This means that the expression of miR-378 would be in parallel with that of PGC1β. PGC1β is known as a regulator of hepatic lipid synthesis and lipoprotein production [22]. It has been reported that the expression of PGC1β is down-regulated in diabetes or obesity, but up-regulated by insulin treatment [23,24]. In contrast, the expression of CYP2E1 is up-regulated in diabetes or obesity, but down-regulated by insulin treatment [25–27]. It would be of interest to investigate the expression of miR-378 in these pathophysiological conditions with reference to the changes in the CYP2E1 expression. In addition, the changes in the expression of miR-378 under the treatment with typical chemical inducers of CYP2E1 *in vivo* or *in vitro* are worth pursuing in the future.

In conclusion, we found that human CYP2E1 expression is regulated by miR-378, mainly via translational repression. This study should provide new insight into the unsolved mechanism of the post-transcriptional regulation of CYP2E1.

Acknowledgements

This work was supported in part by Grant-in-Aid for Scientific Research (B) from Japan Society for the Promotion of Science. We acknowledge Mr. Brent Bell for reviewing the manuscript.

References

[1] Lu Y, Cederbaum AI. CYP2E1 and oxidative liver injury by alcohol. Free Radic Biol Med 2008;44:723–38.
[2] Bolt HM, Roos PH, Thier R. The cytochrome P-450 isoenzyme CYP2E1 in the biological processing of industrial chemicals: consequences for occupational and environmental medicine. Int Arch Occup Environ Health 2003;76:174–85.
[3] Song BJ, Gelboin HV, Park SS, Yang CS, Gonzalez FJ. Complementary DNA and protein sequences of ethanol-inducible rat and human cytochrome P-450s. Transcriptional and post-transcriptional regulation of the rat enzyme. J Biol Chem 1986;261:16689–97.
[4] Song BJ, Matsunaga T, Hardwick JP, Park SS, Veech RL, Yang CS, et al. Stabilization of cytochrome P450j messenger ribonucleic acid in the diabetic rat. Mol Endocrinol 1987;1:542–7.
[5] Roberts BJ, Song BJ, Soh Y, Park SS, Shoaf SE. Ethanol induces CYP2E1 by protein stabilization. Role of ubiquitin conjugation in the rapid degradation of CYP2E1. J Biol Chem 1995;270:29632–5.
[6] Sumida A, Kinoshita K, Fukuda T, Matsuda H, Yamamoto I, Inaba T, et al. Relationship between mRNA levels quantified by reverse transcription-competitive PCR and metabolic activity of CYP3A4 and CYP2E1 in human liver. Biochem Biophys Res Commun 1999;262:499–503.
[7] Bièche I, Narjoz C, Asselah T, Vacher S, Marcellin P, Lidereau R, et al. Reverse transcriptase-PCR quantification of mRNA levels from cytochrome (CYP)1, CYP2 and CYP3 families in 22 different human tissues. Pharmacogenet Genomics 2007;17:731–42.
[8] Shimada T, Yamazaki H, Mimura M, Inui Y, Guengerich FP. Interindividual variations in human liver cytochrome P-450 enzymes involved in the oxida-

tion of drugs, carcinogens and toxic chemicals: studies with liver microsomes of 30 Japanese and 30 Caucasians. J Pharmacol Exp Ther 1994;270:414–23.
[9] Bartel DP. MicroRNAs: genomics, biogenesis, mechanism, and function. Cell 2004;116:281–97.
[10] Ambros V. The functions of animal microRNAs. Nature 2004;431:350–5.
[11] Calin GA, Sevignani C, Dumitru CD, Hyslop T, Noch E, Yendamuri S, et al. Human microRNA genes are frequently located at fragile sites and genomic regions involved in cancers. Proc Natl Acad Sci USA 2004;101:2999–3004.
[12] Lu J, Getz G, Miska EA, Alvarez-Saavedra E, Lamb J, Peck D, et al. MicroRNA expression profiles classify human cancers. Nature 2005;435:834–8.
[13] Lewis BP, Burge CB, Bartel DP. Conserved seed pairing, often flanked by adenosines, indicates that thousands of human genes are microRNA targets. Cell 2005;120:15–20.
[14] Izukawa T, Nakajima M, Fujiwara R, Yamanaka H, Fukami T, Takamiya M, et al. Quantitative analysis of UDP-glucuronosyltransferase (UGT) 1A and UGT2B expression levels in human livers. Drug Metab Dispos 2009;37:1759–68.
[15] Tabata T, Katoh M, Tokudome S, Hosokawa M, Chiba K, Nakajima M, et al. Bioactivation of capecitabine in human liver: involvement of the cytosolic enzyme on 5′-deoxy-5-fluorocytidine formation. Drug Metab Dispos 2004;32:762–7.
[16] Tsuchiya Y, Nakajima M, Kyo S, Kanaya T, Inoue M, Yokoi T. Human CYP1B1 is regulated by estradiol via estrogen receptor. Cancer Res 2004;64:3119–25.
[17] Griffiths-Jones S. The microRNA registry. Nucleic Acids Res 2004;32:D109–11.
[18] Rehmsmeier M, Steffen P, Hochsmann M, Giegerich R. Fast and effective prediction of microRNA/target duplexes. RNA 2004;10:1507–17.
[19] Song BJ, Veech RL, Park SS, Gelboin HV, Gonzalez FJ. Induction of rat hepatic *N*-nitrosodimethylamine demethylase by acetone is due to protein stabilization. J Biol Chem 1989;264:3568–72.
[20] Lee DY, Deng Z, Wang CH, Yang BB. MicroRNA-378 promotes cell survival, tumor growth, and angiogenesis by targeting SuFu and Fus-1 expression. Proc Natl Acad Sci USA 2007;104:20350–5.
[21] Hua Z, Lv Q, Ye W, Wong CK, Cai G, Gu D, et al. MiRNA-directed regulation of VEGF and other angiogenic factors under hypoxia. PLoS ONE 2006;1:e116.
[22] Lin J, Yang R, Tarr PT, Wu PH, Handschin C, Li S, et al. Hyperlipidemic effects of dietary saturated fats mediated through PGC-1β coactivation of SREBP. Cell 2005;120:261–73.
[23] Crunkhorn S, Dearie F, Mantzoros C, Gami H, da Silva WS, Espinoza D, et al. Peroxisome proliferator activator receptor γ coactivator-1 expression is reduced in obesity: potential pathogenic role of saturated fatty acids and p38 mitogen-activated protein kinase activation. J Biol Chem 2007;282:15439–50.
[24] Liu HY, Yehuda-Shnaidman E, Hong T, Han J, Pi J, Liu Z, et al. Prolonged exposure to insulin suppresses mitochondrial production in primary hepatocytes. J Biol Chem 2009;284:14087–95.
[25] Wang Z, Hall SD, Maya JF, Li L, Asghar A, Gorski JC. Diabetes mellitus increases the in vivo activity of cytochrome P450 2E1 in humans. Br J Clin Pharmacol 2003;55:77–85.
[26] De Waziers I, Garlatti M, Bouguet J, Beaune PH, Barouki R. Insulin down-regulates cytochrome P450 2B and 2E expression at the post-transcriptional level in the rat hepatoma cell line. Mol Pharmacol 1995;47:474–9.
[27] Woodcroft KJ, Hafner MS, Novak RF. Insulin signaling in the transcriptional and posttranscriptional regulation of CYP2E1 expression. Hepatology 2002;35:263–73.

Toxicology 275 (2010) 50–57

Contents lists available at ScienceDirect

Toxicology

journal homepage: www.elsevier.com/locate/toxicol

Interleukin-17 is involved in α-naphthylisothiocyanate-induced liver injury in mice

Masanori Kobayashi[a], Satonori Higuchi[a], Katsuhiko Mizuno[a], Koichi Tsuneyama[b], Tatsuki Fukami[a], Miki Nakajima[a], Tsuyoshi Yokoi[a,*]

[a] Drug Metabolism and Toxicology, Faculty of Pharmaceutical Sciences, Kanazawa University, Kakuma-machi, Kanazawa 920-1192, Japan
[b] Department of Diagnostic Pathology, Graduate School of Medicine and Pharmaceutical Science for Research, University of Toyama, Sugitani, Toyama 930-0194, Japan

ARTICLE INFO

Article history:
Received 2 April 2010
Received in revised form 23 May 2010
Accepted 31 May 2010
Available online 8 June 2010

Keywords:
Drug-induced liver injury
Cytokines
MIP-2
Neutrophils
Helper T cells

ABSTRACT

Drug-induced liver injury (DILI) is a major safety concern in drug development and clinical drug therapy. The pathogenesis of DILI usually involves the participation of the parent drug or metabolites that either directly affect the cell biochemistry or elicit an immune response. However, in most cases the mechanisms are unknown. Alpha-naphthylisothiocyanate (ANIT) is known as a hepatotoxicant that causes biliary cell and hepatocyte damage and induces intense neutrophil infiltration in the liver. To investigate whether an immune-mediated mechanism is involved in ANIT-induced liver injury, we examined the plasma AST, ALT and T-Bil levels, hepatic expression of transcriptional factors, cytokines and CXC chemokine genes, plasma IL-17 level and histopathological changes in liver after ANIT administration in mice. Hepatic mRNA expression of retinoid related orphan receptor γt (RORγt) and macrophage inflammatory protein (MIP-2) and plasma IL-17 level was significantly increased in ANIT-administered mice as well as the plasma AST, ALT and T-Bil. Neutralization of IL-17 using anti-IL-17 antibody (100 μg/mouse, single i.p.) suppressed the hepatotoxic effect of ANIT. Co-administration of recombinant IL-17 (1 μg/mouse, single i.p.) to ANIT-administered mice resulted in a remarkable increase of the plasma AST, ALT and T-Bil levels. In conclusion, it was firstly demonstrated that IL-17 is involved in the ANIT-induced liver injury in mice.
© 2010 Elsevier Ireland Ltd. All rights reserved.

1. Introduction

Drug-induced liver injury (DILI) is a major reason for the withdrawal of approved drugs from the market. Some drugs such as tienilic acid, amodiaquine and halothane induce hepatic hypersensitivity reactions (Bugelski, 2005). The pathogenesis of drug-induced liver injury usually involves the participation of the parent drug or metabolites that either directly affect the cell biochemistry or elicit an immune response. In most cases, the mechanisms of DILI are still unknown and predictive experimental animal models are lacking.

Helper T cells (Th cells) are an important regulator of acquired immunity. Th cells are subdivided into Th1, Th2, regulatory T cells (Treg) and Th17 by their unique production of cytokines and characteristic transcription factors (Kidd, 2003; Zhu and Paul, 2008). Th1 cells mediate immune responses against intracellular pathogens and play an important role in resistance to mycobacterial infections. Th2 cells mediate host defense against extracellular parasites and are important in the induction and persistence of asthma and other allergic disease. Treg cells play a critical role in maintaining self-tolerance as well as in regulating immune responses (Zhu and Paul, 2008). Th17 cells, which mainly produce IL-17, play critical roles in the protection against microbial challenges and the induction of autoimmune diseases, and IL-17 can induce many inflammatory cytokines and CXC chemokines (such as MIP-2 and keratinocyte-derived chemokine) resulting in neutrophil infiltration and activation (Zhu and Paul, 2008). One of the causes of DILI is thought to be related to immune-mediated reactions. We previously reported that IL-17 is involved in halothane-induced liver injury in mice (Kobayashi et al., 2009).

Alpha-naphthylisothiocyanate (ANIT) is known as a hepatotoxicant that causes hepatocyte and biliary cell damage and is used in rodents as a model of human intrahepatic cholestasis. ANIT is conjugated with glutathione (GSH) in hepatocytes (Carpenter-Deyo et al., 1991). The GSH–ANIT conjugate is transported by the canalicular efflux transporter, multidrug resistance-associated protein 2 (Mrp2) into bile, and there dissociates into free GSH and ANIT (Dietrich et al., 2001). The reuptake of ANIT in bile by hepatocytes leads to high concentrations of ANIT in the biliary cells. This repetitive round of secretion and reuptake contributes to the hepatotoxicity directly (Dietrich et al., 2001; Jean and Roth, 1995).

* Corresponding author. Tel.: +81 76 234 4407; fax: +81 76 234 4407.
E-mail address: tyokoi@kenroku.kanazawa-u.ac.jp (T. Yokoi).

0300-483X/$ – see front matter © 2010 Elsevier Ireland Ltd. All rights reserved.
doi:10.1016/j.tox.2010.05.011